Figure 1. Angiogenesis-induced myocardial hypertrophy. An increase in capillary mass leads to increased production and release of endothelium-derived NO. NO promotes proteasomal degradation of regulator of G-protein signaling 4 (RGS4), and, thereby, relieves G protein-coupled receptor (GPCR)–mediated hypertrophic signaling involving the phosphatidylinositol 3-kinase (PI3Kγ)/Akt/mammalian target of rapamycin C1 (mTORC1) pathway.

VEGF is a critical angiogenic factor, which is essential for coordinated myocardial angiogenesis in pressure-overloaded hearts.

GATA4, a cardiac-enriched zinc finger transcription factor,[30] plays important roles both in cardiac hypertrophy[31] and in myocardial angiogenesis (Figure 2).[32] GATA4 was abundantly expressed in cardiomyocytes from early embryonic stages, regulated cardiac-specific gene expression, and was downregulated in adult hearts.[30] However, GATA4 was reused when the heart is under stress conditions.[33] Analyses of cardiac-specific GATA4-deleted mice highlighted its important roles in hypertrophic growth, stress responses, and survival of cardiac myocytes in adulthood.[31,34] Furthermore, cardiomyocyte-specific overexpression of GATA4 in the adult heart increased capillary density in the myocardium, whereas myocyte-specific deletion of GATA4 resulted in rarefaction of myocardial capillaries.[32] In addition, overexpression of
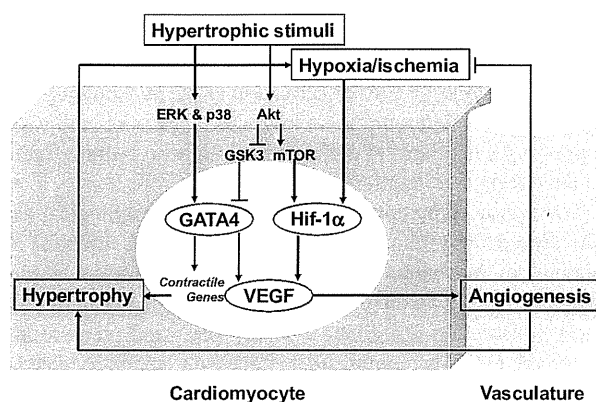

Figure 2. Hypertrophic responses induce myocardial angiogenesis. Hypertrophic stimuli activate intracellular signaling and transcription factors, such as GATA4 and Hif-1. GATA4 induces the gene expression of structural and contractile proteins, resulting in hypertrophy. Hif-1 is also activated by relative hypoxia/ischemia of the hypertrophied myocardium, and Hif-1 transactivates VEGF gene expression to induce angiogenesis. GSK indicates glycogen synthase kinase; mTOR, mammalian target of rapamycin; and VEGF, vascular endothelial growth factor.

GATA4 in cardiac myocytes increased VEGF-A secretion and enhanced angiogenesis in a paracrine manner. The Vegf-A gene promoter has GATA-binding sites and was transactivated by GATA4.[32] However, sustained pathological stimuli suppressed GATA4 levels, which might have contributed to the reduction of capillary numbers in the failing heart.[32] Therefore, GATA4 is involved in the transcriptional regulation of both myocyte hypertrophy and angiogenesis in the heart under stress conditions.

Molecular Mechanisms of Transition From Compensated to Decompensated Hypertrophy

Complex pathophysiological changes have been reported to occur in hypertrophied hearts, including suppressed angiogenesis, vascular rarefaction,[9,10] endothelial dysfunction,[35,36] ventricular dilation and remodeling,[37,38] and fibrosis, which physically hamper oxygen diffusion.[39] These complex changes predispose the myocardium to advanced hypoxia/ischemia. For example, progression of heart failure was related to NO imbalance and endothelial dysfunction, and dysregulation of coronary circulation resulted from altered endothelial function.[40] NO reduction in heart failure influenced endothelial progenitor cells, impairing endothelial repair and regeneration.[41]

The action of VEGF is mainly mediated by 2 receptor tyrosine kinases: VEGF receptor 1 (VEGFR-1, also known as FMS-like tyrosine kinase 1) and VEGFR-2 (also known as Flk-1/kinase insert domain protein receptor).[42] VEGFR-1 and its soluble form VEGFR-1[43] were upregulated in the heart, and soluble form of VEGFR-1 prevented capillary growth by trapping VEGF in pressure-overloaded hearts of rats.[44] Inhibition of soluble form of VEGFR-1 by PlGF, which caused the release of VEGF, was sufficient to induce angiogenesis and to provide cardioprotective effects.[44] These results suggest that soluble form of VEGFR-1 is one of the causative factors inhibiting myocardial angiogenesis, and that VEGF is needed to maintain angiogenesis and cardiac function.

Suppression of capillary density and angiogenesis in the myocardium has been observed in the transition from compensated hypertrophy to decompensated heart failure.[27] In the pressure-overloaded heart, the myocardium becomes ischemic, and the DNA-binding activity of hypoxia inducible factor-1 (Hif-1) increased significantly.[27] Hif-1 is a transcription factor that is stabilized in hypoxic conditions to transactivate various genes encoding hypoxia- and angiogenesis-associated proteins, such as VEGF (Figure 2) and erythropoietin.[45–47] However, in the course of prolonged pathological hypertrophy, Hif-1 and VEGF were downregulated despite persistent myocardial hypoxia in the hypertrophied myocardium.[27] This mismatch of Hif-1 downregulation in pathologically hypertrophied hearts is one of the critical mechanisms that underlies exacerbated myocardial hypoxia and accelerated myocardial damage and dysfunction.

Suppression of Hif-1 in the Hypoxic Myocardium in the Failing Heart

We have recently reported that transformation-related protein 53 (p53), a tumor suppressor protein, was critically involved in this paradoxical downregulation of Hif-1 in

pressure-overloaded hearts.[27] Significant accumulation of p53 was observed in hypertrophied myocardium (Figure 3).[27] Low levels of intracellular p53 were maintained in cardiac myocytes by degradation through the ubiquitin-proteasomal pathway, involving E3 ubiquitin ligases, such as transformed mouse 3T3 cell double minute 2 (MDM2).[48,49] However, p53 accumulated in cardiac myocytes in response to adriamycin-induced genotoxic stress[50] and in response to hypoxic stress induced by pressure overload or MI.[27,51] We also observed p53 accumulation in a mouse model of human dilated cardiomyopathy[52] and in adriamycin-induced cardiomyopathy.[50] These observations suggest that p53 accumulation in the heart is a critical part of the common transition from a functionally healthy heart to heart failure. In general, p53 degradation is mediated by MDM2-dependent ubiquitination, and mRNA expression of MDM2 is positively regulated by p53 in a negative-feedback loop.[48,49] However, p53 accumulation in the failing heart occurs through various molecular mechanisms. For example, in adriamycin-treated hearts, p53 levels were elevated in response to reactive oxygen species–mediated indirect genomic DNA damage.[50] DNA damage activates the DNA damage response pathway, in which phosphorylated ataxia telangiectasia mutated kinase phosphorylates p53 at its amino terminus, thus, stabilizing p53 by inhibiting MDM2 binding.[53] Another trigger for p53 accumulation was hypoxia in cardiac myocytes and nonmyocytes,[54,55] the mechanism of which differs from that of p53 accumulation induced by other stresses, such as DNA damage.[56] Hif-1 was required for hypoxia-induced p53 accumulation and induced p53-dependent transcription via direct binding to p53.[57] In the heart, we identified the carboxyl terminus of heat shock cognate protein 70–interacting protein (CHIP) as one of the E3 ubiquitin ligases required for p53 degradation.[51] CHIP, originally isolated as a cochaperone of heat shock cognate protein 70, had ubiquitin ligase activity, which was attributed to its U-box domain. Although expression of CHIP was not induced by p53 to form a negative-feedback loop-like MDM2, CHIP expression was closely related to p53 expression in cardiomyocytes under hypoxic conditions.[51] We also revealed that Hif-1 mediated suppression of mRNA transcription of CHIP under hypoxic conditions, and that transcriptional suppression

of CHIP mRNA was responsible for p53 accumulation in cardiac myocytes under hypoxia and in infarcted hearts of mice.[51] However, in pressure-overloaded hearts, transcriptional suppression of CHIP mRNA by Hif-1 was not observed, and further investigations are needed to clarify molecular mechanisms underlying p53 accumulation in the failing heart.

Considering these previous reports, what are the functional roles of accumulated p53 in heart failure? Two major roles of p53 are (1) cell cycle arrest[53] and (2) inhibition of blood vessel formation.[58] In response to severe cellular damage, p53 arrests proliferative cells in the G_1 stage of the cell cycle to induce apoptosis or senescence. Although cardiac myocytes do not proliferate after birth, accumulation of p53 induced apoptotic cell death in cardiac myocytes.[55] In hearts, in vivo chemical inhibition of p53 accumulation or transcriptional activity mitigated adriamycin-induced cardiomyopathy[50,59] and heart failure after MI.[51,55] However, previous studies using p53 knockout mice revealed that functional significance of p53 in the regulation of myocyte apoptosis differed according to the disease models. For example, genetic deletion of p53 prevented myocyte apoptosis and cardiac dysfunction in mouse model of heart failure induced by adriamycin treatment,[60] mutation of cardiac α-actin gene (Actc1),[52] and pressure overload.[27] However, p53 deletion did not affect apoptosis of cardiac myocytes in mouse model of heart failure induced by coronary artery ligation.[61]

In the pathological hypertrophied heart, p53 elevation in the myocardium attenuated capillary formation by inhibiting the transcriptional activity of Hif-1 (Figure 3).[27] The expression level of Hif-1mRNA and transcriptional activity of Hif-1 were increased in pressure-overloaded hearts, possibly because of reduced oxygen supply in the hypertrophied myocardium. Activated Hif-1 promoted angiogenesis to prevent progression of hypoxia and maintained functional homeostasis of the myocardium. However, sustained accumulation of p53, by an undefined mechanism, inhibited the transcriptional activity of Hif-1 and, thereby, promoted progression of maladaptive heart failure.[27] These findings indicate that p53 plays pivotal and pathogenic roles in the progression of heart failure via various pathways, including apoptotic cell death and suppression of angiogenesis in the heart.

Hypertrophied Heart

Relative Hypoxia

VEGF

Maintained angiogenesis by VEGF

Failing Heart

Advanced Hypoxia

Reduced angiogenesis by p53 accumulation
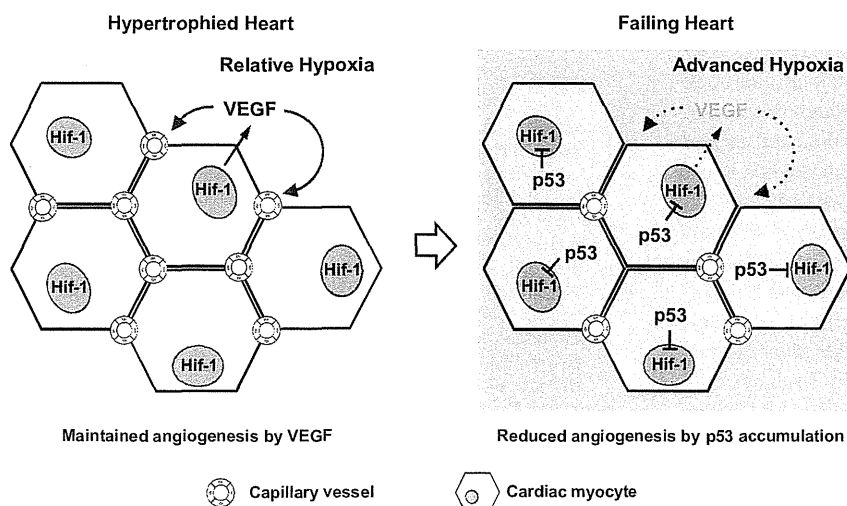
Capillary vessel   Cardiac myocyte

Figure 3. Suppression of hypoxia inducible factor-1 (Hif-1) by transformation-related protein 53 (p53) in the hypoxic failing heart. In the hypertrophied heart, myocardial angiogenesis is maintained by vascular endothelial growth factor (VEGF), which is induced by Hif-1 in relative hypoxic conditions. However, in the advanced hypoxic condition of the failing heart, Hif-1 is inhibited by p53 accumulation in the myocardium, resulting in the suppression of myocardial angiogenesis and cardiac dysfunction.

Therapeutic Myocardial Angiogenesis as a Potential Therapy for Heart Failure

In hearts manifesting pathological hypertrophy, the capillary density decreased during the transition from cardiac hypertrophy to heart failure.[62] This phenomenon is clinically relevant because an intravascular ultrasound study demonstrated that coronary flow reserve was reduced in patients with hypertension with left ventricular hypertrophy when compared with those without left ventricular hypertrophy.[63] The change of coronary angiogenesis also accompanies cardiac hypertrophy not resulting from pressure overload. When capillary patterns were studied in histological sections, a significant decrease in capillary density was observed in the hearts of patients with dilated cardiomyopathy, ischemic cardiomyopathy, or inflammatory cardiomyopathy.[64] On the basis of these experimental and clinical observations, we found that the therapeutic myocardial angiogenesis is emerging as a promising approach for the prevention and treatment of heart failure.[65]

Several strategies to enhance myocardial angiogenesis have been investigated, including delivery of angiogenic genes or growth factors. The candidate angiogenic factors include VEGF-A,[66–69] VEGF-B,[70–72] fibroblast growth factor-2,[68,73,74] fibroblast growth factor-5,[75,76] stromal cell-derived factor-1,[77,78] hepatocyte growth factor,[79] and midkine.[80] Although long-term stimulation with VEGF-A promoted immature angiogenesis and increased vascular permeability,[81] simultaneous stimulation with VEGF-A and angiopoietin-1 yielded coordinated vascular growth and improved cardiac perfusion and function in rodent[69,82] and porcine[83] models of MI. A combination of fibroblast growth factor-2 and hepatocyte growth factor synergistically stimulated angiogenesis and prevented progression of heart failure in a rat model of MI.[84] To improve the efficacy and safety of the therapeutic interventions for myocardial angiogenesis, further studies are required to determine the optimal combination of angiogenic growth factors and to improve the technology of delivery methods to the myocardium.

One of the potential therapeutic targets is Hif-1, a key transcriptional regulator for the hypoxic induction of angiogenic growth factors.[47] Cobalt is known to stabilize Hif-1α and prevent the decline of contractile function in perfused rat hearts under hypoxia-reoxygenation.[85] According to recent studies, cobalt-induced stabilization of Hif-1α is dependent on copper.[86,87] Furthermore, copper supplementation reversed contractile dysfunction and prevented transition to heart failure in pressure-overloaded mice, at least in part through promotion of myocardial angiogenesis.[88] In addition to cobalt and copper function, several approved drugs have been reported to affect myocardial angiogenesis. For example, pitavastatin induced myocardial angiogenesis and prevented progression of heart failure in pressure-overloaded mice.[89] The calcium channel blocker, benidipine, increased capillary density and reduced left ventricular stiffness in Dahl salt-sensitive rats.[90] Although the promotion of myocardial angiogenesis needs much further study before it becomes an established remedy for heart failure patients, a certain amount of preclinical evidence has been accumulated, and the translation of this concept into clinical practice will likely continue in a steady progression in the years to come.

Conclusions

In this review, we summarize the functional association between cardiac hypertrophy and myocardial angiogenesis at molecular and cellular levels. We also discuss dysregulation of capillary angiogenesis in the hypertrophied heart in relation to the transitional process from compensated hypertrophy to decompensated heart failure. Accumulated experimental data provide insights about potential therapeutic strategies for heart diseases. It may be advantageous to stimulate angiogenesis to prevent or reverse heart failure in general or to treat heart failure with a combination of antihypertrophic and proangiogenic agents. However, we still have an array of unanswered questions about an integrative understanding of cardiac hypertrophy and angiogenesis in physiological and pathological conditions. Although it is well established that neurohumoral factors, mechanical and oxidative stresses, metabolic changes, and DNA damage are accompanied by cardiac dysfunction, precise triggers and mechanisms for the disruption of coordinated angiogenesis remain unclear. At the cellular level, it is still unclear how cardiomyocytes, endothelial cells, fibroblasts, and smooth muscle cells coordinate myocardial hypertrophy and angiogenesis in response to environmental changes. Furthermore, experimental studies in this field have been performed mainly using pressure overload and MI, but there is less information about dilated cardiomyopathy or other types of heart failure. Although in theory we consider combination therapy for antihypertrophy and proangiogenesis to be promising, potential molecular targets and mechanisms are still unknown. Further investigations with multidisciplinary approaches would be necessary to resolve these challenging questions and to clarify the whole picture comprised the inextricable link between hypertrophy and angiogenesis in the heart.

Sources of Funding

Disclosures

None.

References

1. Srivastava D, Olson EN. A genetic blueprint for cardiac development. *Nature*. 2000;407:221–226.
2. Luttun A, Carmeliet P. De novo vasculogenesis in the heart. *Cardiovasc Res*. 2003;58:378–389.
3. Riley PR, Smart N. Vascularizing the heart. *Cardiovasc Res*. 2011;91:260–268.
4. Maillet M, van Berlo JH, Molkentin JD. Molecular basis of physiological heart growth: fundamental concepts and new players. *Nat Rev Mol Cell Biol*. 2013;14:38–48.
5. van Berlo JH, Maillet M, Molkentin JD. Signaling effectors underlying pathologic growth and remodeling of the heart. *J Clin Invest*. 2013;123:37–45.
6. Souders CA, Bowers SL, Baudino TA. Cardiac fibroblast: the renaissance cell. *Circ Res*. 2009;105:1164–1176.
7. Anversa P, Levicky V, Beghi C, McDonald SL, Kikkawa Y. Morphometry of exercise-induced right ventricular hypertrophy in the rat. *Circ Res*. 1983;52:57–64.

8. Anversa P, Capasso JM. Loss of intermediate-sized coronary arteries and capillary proliferation after left ventricular failure in rats. *Am J Physiol.* 1991;260:H1552–H1560.

9. Anversa P, Capasso JM, Ricci R, Sonnenblick EH, Olivetti G. Morphometric analysis of coronary capillaries during physiologic myocardial growth and induced cardiac hypertrophy: a review. *Int J Microcirc Clin Exp.* 1989;8:353–363.

10. Beltrami CA, Finato N, Rocco M, Feruglio GA, Puricelli C, Cigola E, Quaini F, Sonnenblick EH, Olivetti G, Anversa P. Structural basis of end-stage failure in ischemic cardiomyopathy in humans. *Circulation.* 1994;89:151–163.

11. Dor Y, Djonov V, Abramovitch R, Itin A, Fishman GI, Carmeliet P, Goelman G, Keshet E. Conditional switching of VEGF provides new insights into adult neovascularization and pro-angiogenic therapy. *EMBO J.* 2002;21:1939–1947.

12. Jaba IM, Zhuang ZW, Li N, Jiang Y, Martin KA, Sinusas AJ, Papademetris X, Simons M, Sessa WC, Young LH, Tirziu D. NO triggers RGS4 degradation to coordinate angiogenesis and cardiomyocyte growth. *J Clin Invest.* 2013;123:1718–1731.

13. Tirziu D, Chorianopoulos E, Moodie KL, Palac RT, Zhuang ZW, Tjwa M, Roncal C, Eriksson U, Fu Q, Elfenbein A, Hall AE, Carmeliet P, Moons L, Simons M. Myocardial hypertrophy in the absence of external stimuli is induced by angiogenesis in mice. *J Clin Invest.* 2007;117:3188–3197.

14. Accornero F, van Berlo JH, Benard MJ, Lorenz JN, Carmeliet P, Molkentin JD. Placental growth factor regulates cardiac adaptation and hypertrophy through a paracrine mechanism. *Circ Res.* 2011;109:272–280.

15. Lambert NA, Johnston CA, Cappell SD, Kuravi S, Kimple AJ, Willard FS, Siderovski DP. Regulators of G-protein signaling accelerate GPCR signaling kinetics and govern sensitivity solely by accelerating GTPase activity. *Proc Natl Acad Sci U S A.* 2010;107:7066–7071.

16. Hudlicka O, Brown M, Egginton S. Angiogenesis in skeletal and cardiac muscle. *Physiol Rev.* 1992;72:369–417.

17. Dallabrida SM, Ismail NS, Pravda EA, Parodi EM, Dickie R, Durand EM, Lai J, Cassiola F, Rogers RA, Rupnick MA. Integrin binding angiopoietin-1 monomers reduce cardiac hypertrophy. *FASEB J.* 2008;22:3010–3023.

18. Kardami E, Detillieux K, Ma X, Jiang Z, Santiago JJ, Jimenez SK, Cattini PA. Fibroblast growth factor-2 and cardioprotection. *Heart Fail Rev.* 2007;12:267–277.

19. Dobaczewski M, Chen W, Frangogiannis NG. Transforming growth factor (TGF)-β signaling in cardiac remodeling. *J Mol Cell Cardiol.* 2011;51:600–606.

20. Andrae J, Gallini R, Betsholtz C. Role of platelet-derived growth factors in physiology and medicine. *Genes Dev.* 2008;22:1276–1312.

21. Shiojima I, Yefremashvili M, Luo Z, Kureishi Y, Takahashi A, Tao J, Rosenzweig A, Kahn CR, Abel ED, Walsh K. Akt signaling mediates postnatal heart growth in response to insulin and nutritional status. *J Biol Chem.* 2002;277:37670–37677.

22. Matsui T, Nagoshi T, Rosenzweig A. Akt and PI 3-kinase signaling in cardiomyocyte hypertrophy and survival. *Cell Cycle.* 2003;2:220–223.

23. Kemi OJ, Ceci M, Wisloff U, Grimaldi S, Gallo P, Smith GL, Condorelli G, Ellingsen O. Activation or inactivation of cardiac Akt/mTOR signaling diverges physiological from pathological hypertrophy. *J Cell Physiol.* 2008;214:316–321.

24. Shiojima I, Sato K, Izumiya Y, Schiekofer S, Ito M, Liao R, Colucci WS, Walsh K. Disruption of coordinated cardiac hypertrophy and angiogenesis contributes to the transition to heart failure. *J Clin Invest.* 2005;115:2108–2118.

25. Phung TL, Ziv K, Dabydeen D, et al. Pathological angiogenesis is induced by sustained Akt signaling and inhibited by rapamycin. *Cancer Cell.* 2006;10:159–170.

26. Miyachi M, Yazawa H, Furukawa M, Tsuboi K, Ohtake M, Nishizawa T, Hashimoto K, Yokoi T, Kojima T, Murate T, Yokota M, Murohara T, Koike Y, Nagata K. Exercise training alters left ventricular geometry and attenuates heart failure in dahl salt-sensitive hypertensive rats. *Hypertension.* 2009;53:701–707.

27. Sano M, Minamino T, Toko H, et al. p53-induced inhibition of Hif-1 causes cardiac dysfunction during pressure overload. *Nature.* 2007;446:444–448.

28. Izumiya Y, Shiojima I, Sato K, Sawyer DB, Colucci WS, Walsh K. Vascular endothelial growth factor blockade promotes the transition from compensatory cardiac hypertrophy to failure in response to pressure overload. *Hypertension.* 2006;47:887–893.

29. Friehs I, Barillas R, Vasilyev NV, Roy N, McGowan FX, del Nido PJ. Vascular endothelial growth factor prevents apoptosis and preserves contractile function in hypertrophied infant heart. *Circulation.* 2006;114:I290–I295.

30. Molkentin JD. The zinc finger-containing transcription factors GATA-4, -5, and -6. Ubiquitously expressed regulators of tissue-specific gene expression. *J Biol Chem.* 2000;275:38949–38952.

31. Oka T, Maillet M, Watt AJ, Schwartz RJ, Aronow BJ, Duncan SA, Molkentin JD. Cardiac-specific deletion of Gata4 reveals its requirement for hypertrophy, compensation, and myocyte viability. *Circ Res.* 2006;98:837–845.

32. Heineke J, Auger-Messier M, Xu J, Oka T, Sargent MA, York A, Klevitsky R, Vaikunth S, Duncan SA, Aronow BJ, Robbins J, Crombleholme TM, Cromblehol TM, Molkentin JD. Cardiomyocyte GATA4 functions as a stress-responsive regulator of angiogenesis in the murine heart. *J Clin Invest.* 2007;117:3198–3210.

33. Oka T, Xu J, Molkentin JD. Re-employment of developmental transcription factors in adult heart disease. *Semin Cell Dev Biol.* 2007;18:117–131.

34. Bisping E, Ikeda S, Kong SW, Tarnavski O, Bodyak N, McMullen JR, Rajagopal S, Son JK, Ma Q, Springer Z, Kang PM, Izumo S, Pu WT. Gata4 is required for maintenance of postnatal cardiac function and protection from pressure overload-induced heart failure. *Proc Natl Acad Sci U S A.* 2006;103:14471–14476.

35. Bauersachs J, Widder JD. Endothelial dysfunction in heart failure. *Pharmacol Rep.* 2008;60:119–126.

36. Marti CN, Gheorghiade M, Kalogeropoulos AP, Georgiopoulou VV, Quyyumi AA, Butler J. Endothelial dysfunction, arterial stiffness, and heart failure. *J Am Coll Cardiol.* 2012;60:1455–1469.

37. Kemp CD, Conte JV. The pathophysiology of heart failure. *Cardiovasc Pathol.* 2012;21:365–371.

38. Gaasch WH, Zile MR. Left ventricular structural remodeling in health and disease: with special emphasis on volume, mass, and geometry. *J Am Coll Cardiol.* 2011;58:1733–1740.

39. De Boer RA, Pinto YM, Van Veldhuisen DJ. The imbalance between oxygen demand and supply as a potential mechanism in the pathophysiology of heart failure: the role of microvascular growth and abnormalities. *Microcirculation.* 2003;10:113–126.

40. Treasure CB, Vita JA, Cox DA, Fish RD, Gordon JB, Mudge GH, Colucci WS, Sutton MG, Selwyn AP, Alexander RW. Endothelium-dependent dilation of the coronary microvasculature is impaired in dilated cardiomyopathy. *Circulation.* 1990;81:772–779.

41. Aicher A, Heeschen C, Mildner-Rihm C, Urbich C, Ihling C, Technau-Ihling K, Zeiher AM, Dimmeler S. Essential role of endothelial nitric oxide synthase for mobilization of stem and progenitor cells. *Nat Med.* 2003;9:1370–1376.

42. Ferrara N. Role of vascular endothelial growth factor in the regulation of angiogenesis. *Kidney Int.* 1999;56:794–814.

43. Kendall RL, Thomas KA. Inhibition of vascular endothelial cell growth factor activity by an endogenously encoded soluble receptor. *Proc Natl Acad Sci U S A.* 1993;90:10705–10709.

44. Kaza E, Ablasser K, Poutias D, Griffiths ER, Saad FA, Hofstaetter JG, del Nido PJ, Friehs I. Up-regulation of soluble vascular endothelial growth factor receptor-1 prevents angiogenesis in hypertrophied myocardium. *Cardiovasc Res.* 2011;89:410–418.

45. Forsythe JA, Jiang BH, Iyer NV, Agani F, Leung SW, Koos RD, Semenza GL. Activation of vascular endothelial growth factor gene transcription by hypoxia-inducible factor 1. *Mol Cell Biol.* 1996;16:4604–4613.

46. Grimm C, Wenzel A, Groszer M, Mayser H, Seeliger M, Samardzija M, Bauer C, Gassmann M, Remé CE. HIF-1-induced erythropoietin in the hypoxic retina protects against light-induced retinal degeneration. *Nat Med.* 2002;8:718–724.

47. Semenza GL. Hypoxia-inducible factors in physiology and medicine. *Cell.* 2012;148:399–408.

48. Haupt Y, Maya R, Kazaz A, Oren M. Mdm2 promotes the rapid degradation of p53. *Nature.* 1997;387:296–299.

49. Kubbutat MH, Jones SN, Vousden KH. Regulation of p53 stability by Mdm2. *Nature.* 1997;387:299–303.

50. Yoshida M, Shiojima I, Ikeda H, Komuro I. Chronic doxorubicin cardiotoxicity is mediated by oxidative DNA damage-ATM-p53-apoptosis pathway and attenuated by pitavastatin through the inhibition of Rac1 activity. *J Mol Cell Cardiol.* 2009;47:698–705.

51. Naito AT, Okada S, Minamino T, Iwanaga K, Liu ML, Sumida T, Nomura S, Sahara N, Mizoroki T, Takashima A, Akazawa H, Nagai T, Shiojima I, Komuro I. Promotion of CHIP-mediated p53 degradation protects the heart from ischemic injury. *Circ Res.* 2010;106:1692–1702.

52. Toko H, Takahashi H, Kayama Y, et al. Ca2+/calmodulin-dependent kinase IIdelta causes heart failure by accumulation of p53 in dilated cardiomyopathy. *Circulation.* 2010;122:891–899.

53. Carr AM. Cell cycle. Piecing together the p53 puzzle. *Science.* 2000;287:1765–1766.
54. Liu P, Xu B, Cavalieri TA, Hock CE. Pifithrin-alpha attenuates p53-mediated apoptosis and improves cardiac function in response to myocardial ischemia/reperfusion in aged rats. *Shock.* 2006;26:608–614.
55. Long X, Boluyt MO, Hipolito ML, Lundberg MS, Zheng JS, O'Neill L, Cirielli C, Lakatta EG, Crow MT. p53 and the hypoxia-induced apoptosis of cultured neonatal rat cardiac myocytes. *J Clin Invest.* 1997;99:2635–2643.
56. Graeber TG, Peterson JF, Tsai M, Monica K, Fornace AJ Jr, Giaccia AJ. Hypoxia induces accumulation of p53 protein, but activation of a G1-phase checkpoint by low-oxygen conditions is independent of p53 status. *Mol Cell Biol.* 1994;14:6264–6277.
57. An WG, Kanekal M, Simon MC, Maltepe E, Blagosklonny MV, Neckers LM. Stabilization of wild-type p53 by hypoxia-inducible factor 1alpha. *Nature.* 1998;392:405–408.
58. Muller PA, Vousden KH. p53 mutations in cancer. *Nat Cell Biol.* 2013;15:2–8.
59. Liu X, Chua CC, Gao J, Chen Z, Landy CL, Hamdy R, Chua BH. Pifithrin-alpha protects against doxorubicin-induced apoptosis and acute cardiotoxicity in mice. *Am J Physiol Heart Circ Physiol.* 2004;286:H933–H939.
60. Shizukuda Y, Matoba S, Mian OY, Nguyen T, Hwang PM. Targeted disruption of p53 attenuates doxorubicin-induced cardiac toxicity in mice. *Mol Cell Biochem.* 2005;273:25–32.
61. Bialik S, Geenen DL, Sasson IE, Cheng R, Horner JW, Evans SM, Lord EM, Koch CJ, Kitsis RN. Myocyte apoptosis during acute myocardial infarction in the mouse localizes to hypoxic regions but occurs independently of p53. *J Clin Invest.* 1997;100:1363–1372.
62. Flanagan MF, Fujii AM, Colan SD, Flanagan RG, Lock JE. Myocardial angiogenesis and coronary perfusion in left ventricular pressure-overload hypertrophy in the young lamb. Evidence for inhibition with chronic protamine administration. *Circ Res.* 1991;68:1458–1470.
63. Hamasaki S, Al Suwaidi J, Higano ST, Miyauchi K, Holmes DR Jr, Lerman A. Attenuated coronary flow reserve and vascular remodeling in patients with hypertension and left ventricular hypertrophy. *J Am Coll Cardiol.* 2000;35:1654–1660.
64. Karch R, Neumann F, Ullrich R, Neumüller J, Podesser BK, Neumann M, Schreiner W. The spatial pattern of coronary capillaries in patients with dilated, ischemic, or inflammatory cardiomyopathy. *Cardiovasc Pathol.* 2005;14:135–144.
65. Hou J, Kang YJ. Regression of pathological cardiac hypertrophy: signaling pathways and therapeutic targets. *Pharmacol Ther.* 2012;135:337–354.
66. Losordo DW, Vale PR, Symes JF, Dunnington CH, Esakof DD, Maysky M, Ashare AB, Lathi K, Isner JM. Gene therapy for myocardial angiogenesis: initial clinical results with direct myocardial injection of phVEGF165 as sole therapy for myocardial ischemia. *Circulation.* 1998;98:2800–2804.
67. Pearlman JD, Hibberd MG, Chuang ML, Harada K, Lopez JJ, Gladstone SR, Friedman M, Sellke FW, Simons M. Magnetic resonance mapping demonstrates benefits of VEGF-induced myocardial angiogenesis. *Nat Med.* 1995;1:1085–1089.
68. Hughes GC, Biswas SS, Yin B, Coleman RE, DeGrado TR, Landolfo CK, Lowe JE, Annex BH, Landolfo KP. Therapeutic angiogenesis in chronically ischemic porcine myocardium: comparative effects of bFGF and VEGF. *Ann Thorac Surg.* 2004;77:812–818.
69. Zhou L, Ma W, Yang Z, Zhang F, Lu L, Ding Z, Ding B, Ha T, Gao X, Li C. VEGF165 and angiopoietin-1 decreased myocardium infarct size through phosphatidylinositol-3 kinase and Bcl-2 pathways. *Gene Ther.* 2005;12:196–202.
70. Pepe M, Mamdani M, Zentilin L, Csiszar A, Qanud K, Zacchigna S, Ungvari Z, Puligadda U, Moimas S, Xu X, Edwards JG, Hintze TH, Giacca M, Recchia FA. Intramyocardial VEGF-B167 gene delivery delays the progression towards congestive failure in dogs with pacing-induced dilated cardiomyopathy. *Circ Res.* 2010;106:1893–1903.
71. Serpi R, Tolonen AM, Huusko J, Rysä J, Tenhunen O, Ylä-Herttuala S, Ruskoaho H. Vascular endothelial growth factor-B gene transfer prevents angiotensin II-induced diastolic dysfunction via proliferation and capillary dilatation in rats. *Cardiovasc Res.* 2011;89:204–213.
72. Huusko J, Lottonen L, Merentie M, Gurzeler E, Anisimov A, Miyanohara A, Alitalo K, Tavi P, Ylä-Herttuala S. AAV9-mediated VEGF-B gene transfer improves systolic function in progressive left ventricular hypertrophy. *Mol Ther.* 2012;20:2212–2221.
73. Battler A, Scheinowitz M, Bor A, Hasdai D, Vered Z, Di Segni E, Varda-Bloom N, Nass D, Engelberg S, Eldar M. Intracoronary injection of basic fibroblast growth factor enhances angiogenesis in infarcted swine myocardium. *J Am Coll Cardiol.* 1993;22:2001–2006.
74. Laham RJ, Chronos NA, Pike M, Leimbach ME, Udelson JE, Pearlman JD, Pettigrew RI, Whitehouse MJ, Yoshizawa C, Simons M. Intracoronary basic fibroblast growth factor (FGF-2) in patients with severe ischemic heart disease: results of a phase I open-label dose escalation study. *J Am Coll Cardiol.* 2000;36:2132–2139.
75. Suzuki G, Lee TC, Fallavollita JA, Canty JM Jr. Adenoviral gene transfer of FGF-5 to hibernating myocardium improves function and stimulates myocytes to hypertrophy and reenter the cell cycle. *Circ Res.* 2005;96:767–775.
76. Giordano FJ, Ping P, McKirnan MD, Nozaki S, DeMaria AN, Dillmann WH, Mathieu-Costello O, Hammond HK. Intracoronary gene transfer of fibroblast growth factor-5 increases blood flow and contractile function in an ischemic region of the heart. *Nat Med.* 1996;2:534–539.
77. Sundararaman S, Miller TJ, Pastore JM, Kiedrowski M, Aras R, Penn MS. Plasmid-based transient human stromal cell-derived factor-1 gene transfer improves cardiac function in chronic heart failure. *Gene Ther.* 2011;18:867–873.
78. Kanki S, Segers VF, Wu W, Kakkar R, Gannon J, Sys SU, Sandrasagra A, Lee RT. Stromal cell-derived factor-1 retention and cardioprotection for ischemic myocardium. *Circ Heart Fail.* 2011;4:509–518.
79. Siltanen A, Kitabayashi K, Lakkisto P, Mäkelä J, Pätilä T, Ono M, Tikkanen I, Sawa Y, Kankuri E, Harjula A. hHGF overexpression in myoblast sheets enhances their angiogenic potential in rat chronic heart failure. *PLoS One.* 2011;6:e19161.
80. Sumida A, Horiba M, Ishiguro H, Takenaka H, Ueda N, Ooboshi H, Opthof T, Kadomatsu K, Kodama I. Midkine gene transfer after myocardial infarction in rats prevents remodelling and ameliorates cardiac dysfunction. *Cardiovasc Res.* 2010;86:113–121.
81. Weis SM, Cheresh DA. Pathophysiological consequences of VEGF-induced vascular permeability. *Nature.* 2005;437:497–504.
82. Su H, Takagawa J, Huang Y, Arakawa-Hoyt J, Pons J, Grossman W, Kan YW. Additive effect of AAV-mediated angiopoietin-1 and VEGF expression on the therapy of infarcted heart. *Int J Cardiol.* 2009;133:191–197.
83. Tao Z, Chen B, Tan X, Zhao Y, Wang L, Zhu T, Cao K, Yang Z, Kan YW, Su H. Coexpression of VEGF and angiopoietin-1 promotes angiogenesis and cardiomyocyte proliferation reduces apoptosis in porcine myocardial infarction (MI) heart. *Proc Natl Acad Sci U S A.* 2011;108:2064–2069.
84. Banquet S, Gomez E, Nicol L, Edwards-Lévy F, Henry JP, Cao R, Schapman D, Dautreaux B, Lallemand F, Bauer F, Cao Y, Thuillez C, Mulder P, Richard V, Brakenhielm E. Arteriogenic therapy by intramyocardial sustained delivery of a novel growth factor combination prevents chronic heart failure. *Circulation.* 2011;124:1059–1069.
85. Endoh H, Kaneko T, Nakamura H, Doi K, Takahashi E. Improved cardiac contractile functions in hypoxia-reoxygenation in rats treated with low concentration Co(2+). *Am J Physiol Heart Circ Physiol.* 2000;279:H2713–H2719.
86. Feng W, Ye F, Xue W, Zhou Z, Kang YJ. Copper regulation of hypoxia-inducible factor-1 activity. *Mol Pharmacol.* 2009;75:174–182.
87. Qiu L, Ding X, Zhang Z, Kang YJ. Copper is required for cobalt-induced transcriptional activity of hypoxia-inducible factor-1. *J Pharmacol Exp Ther.* 2012;342:561–567.
88. Jiang Y, Reynolds C, Xiao C, Feng W, Zhou Z, Rodriguez W, Tyagi SC, Eaton JW, Saari JT, Kang YJ. Dietary copper supplementation reverses hypertrophic cardiomyopathy induced by chronic pressure overload in mice. *J Exp Med.* 2007;204:657–666.
89. Kameda Y, Hasegawa H, Kubota A, Tadokoro H, Kobayashi Y, Komuro I, Takano H. Effects of pitavastatin on pressure overload-induced heart failure in mice. *Circ J.* 2012;76:1159–1168.
90. Nishizawa T, Cheng XW, Jin Z, Obata K, Nagata K, Hirashiki A, Sasaki T, Noda A, Takeshita K, Izawa H, Shi GP, Kuzuya M, Okumura K, Murohara T. Ca(2+) channel blocker benidipine promotes coronary angiogenesis and reduces both left-ventricular diastolic stiffness and mortality in hypertensive rats. *J Hypertens.* 2010;28:1515–1526.

LATE BREAKING CLINICAL TRIAL (JCS 2013)

Urgent Management of Rapid Heart Rate in Patients With Atrial Fibrillation/Flutter and Left Ventricular Dysfunction
– Comparison of the Ultra-Short-Acting β1-Selective Blocker Landiolol With Digoxin (J-Land Study) –

Ryozo Nagai, MD, PhD; Koichiro Kinugawa, MD, PhD; Hiroshi Inoue, MD, PhD;
Hirotsugu Atarashi, MD, PhD; Yoshihiko Seino, MD, PhD; Takeshi Yamashita, MD, PhD;
Wataru Shimizu, MD, PhD; Takeshi Aiba, MD, PhD; Masafumi Kitakaze, MD, PhD;
Atsuhiro Sakamoto, MD, PhD; Takanori Ikeda, MD, PhD; Yasushi Imai, MD, PhD;
Takashi Daimon, PhD; Katsuhiro Fujino, MSc; Tetsuji Nagano, MSc;
Tatsuaki Okamura, MSc; Masatsugu Hori, MD, PhD; the J-Land Investigators

Background: A rapid heart rate (HR) during atrial fibrillation (AF) and atrial flutter (AFL) in left ventricular (LV) dysfunction often impairs cardiac performance. The J-Land study was conducted to compare the efficacy and safety of landiolol, an ultra-short-acting β-blocker, with those of digoxin for swift control of tachycardia in AF/AFL in patients with LV dysfunction.

Methods and Results: The 200 patients with AF/AFL, HR ≥120 beats/min, and LV ejection fraction 25–50% were randomized to receive either landiolol (n=93) or digoxin (n=107). Successful HR control was defined as ≥20% reduction in HR together with HR <110 beats/min at 2h after starting intravenous administration of landiolol or digoxin. The dose of landiolol was adjusted in the range of $1-10 \mu g \cdot kg^{-1} \cdot min^{-1}$ according to the patient's condition. The mean HR at baseline was 138.2±15.7 and 138.0±15.0 beats/min in the landiolol and digoxin groups, respectively. Successful HR control was achieved in 48.0% of patients treated with landiolol and in 13.9% of patients treated with digoxin ($P<0.0001$). Serious adverse events were reported in 2 and 3 patients in each group, respectively.

Conclusions: Landiolol was more effective for controlling rapid HR than digoxin in AF/AFL patients with LV dysfunction, and could be considered as a therapeutic option in this clinical setting. (*Circ J* 2013; **77**: 908–916)

Key Words: Atrial fibrillation; Atrial flutter; β-blocker; Landiolol; Left ventricular dysfunction

A trial fibrillation (AF) and atrial flutter (AFL) are common arrhythmias in patients with left ventricular (LV) dysfunction. Over 20% of patients with heart failure exhibit AF.[1,2] In these patients, AF/AFL are often associated with a rapid ventricular response during the worsening of heart failure.[3,4] However, a sustained rapid ventricular response may

Figure 1. Study protocol. *Dose could reduce to 0.125 mg in patients being treated with oral digitalis preparations. **Additional doses of digoxin administered as deemed necessary.

further deteriorate cardiac function,[5] accelerating the symptoms of heart failure.[6–8]

Editorial p 893

Intravenous administration of digoxin is considered the standard therapy for controlling the rapid ventricular response in AF/AFL patients with cardiac dysfunction or heart failure.[4,9] Although digoxin has some beneficial effects for treating heart failure, because of its positive inotropic effects, digoxin may also have a negative chronotropic effect as a result of vagal stimulation that develops much more slowly, often taking several hours to reach the maximal effect.[9,10] Short-acting parenteral β-blockers can act more rapidly than digoxin, and may provide swift control of the heart rate (HR) in these clinical settings. However, there is concern that β-blockers may depress cardiac function and further deteriorate ventricular dysfunction, accelerating heart failure.

Landiolol, an ultra-short-acting β-blocker, is rapidly metabolized to inactive forms in the blood and liver, resulting in a short half-life of approximately 4 min in human blood. In addition, it selectively binds to $\beta 1$ receptors, with a $\beta 1$ receptor selectivity ($\beta 1/\beta 2$) as high as 251.[11] Based on these properties, landiolol has been reported to be useful for treating several acute disorders, including arrhythmias during heart surgery,[12] acute myocardial infarction,[13] acute decompensated heart failure,[14] and refractory electrical storm.[15]

Ultra-short-acting β-blockers may be useful to control the HR with minimal effects on cardiac function because the negative inotropic effect is not sustained after decreasing the dose or stopping administration of these drugs. Therefore, the present study was designed to evaluate the efficacy and safety of intravenous landiolol for achieving rapid control of tachycardia in patients with AF/AFL and LV dysfunction.

Methods

Study Design and Patients
This study was designed as a central registration, prospective, multicenter, single-blind, randomized, parallel-group study for examining tachycardia in patients with AF/AFL and LV dysfunction. It was conducted in 95 hospitals in Japan between March 2011 and August 2012. The main inclusion criteria were: male or female inpatients aged ≥20 years; New York Heart Association (NYHA) class III or IV; and AF/AFL with an LV ejection fraction (EF) of 25–50% and a HR ≥120 beats/min. The main exclusion criteria were: necessity for electrical cardioversion; serious valve stenosis; confirmed or suspected hyperthyroidism; implantable cardiac pacemaker and/or implantable defibrillator; necessity for mechanical ventilation; and cardiogenic shock (systolic blood pressure (BP) <90 mmHg). The use of antiarrhythmic drugs, sympathomimetic drugs, sympatholytic drugs, defibrillator use, catheter ablation, and pacemaker therapy were prohibited from administration until completing all observations at 2 h after starting treatment. However, patients being treated with oral β-blockers (carvedilol or bisoprolol) or oral digitalis preparations for chronic heart failure, chronic AF, and/or chronic AFL could participate in the study under continued treatment without changes in their doses.

The enrolled patients gave informed consent before randomization to either treatment. The study protocol was approved by the institutional review boards at all of the participating institutions, and the study was conducted in accordance with the Declaration of Helsinki.

Study Protocol
The study protocol is shown in Figure 1. After enrolment, each patient was randomized to receive landiolol or digoxin using the permuted block method. In the landiolol group, continuous intravenous administration of landiolol was started at a dose of $1 \mu g \cdot kg^{-1} \cdot min^{-1}$ and titrated to a maximum dose of $10 \mu g \cdot kg^{-1} \cdot min^{-1}$ according to the patient's condition. Landiolol was administered for ≥2 h and up to 72 h. In the digoxin group, digoxin was intravenously administered at an initial dose of 0.25 mg and could be uptitrated within 72 h according to the patient's condition. For patients treated with oral digitalis, the parenteral digoxin dose could be reduced to 0.125 mg according to the patient's condition to prevent digitalis intoxication.

The primary efficacy endpoint was the percentage of patients with both a HR <110 beats/min and ≥20% decrease from baseline at 2 h after administration. The secondary endpoints were HR at 0.5, 1, and 2 h, conversion to normal sinus rhythm, and subjective symptoms and objective findings (palpitations,

Figure 2. Patient disposition.
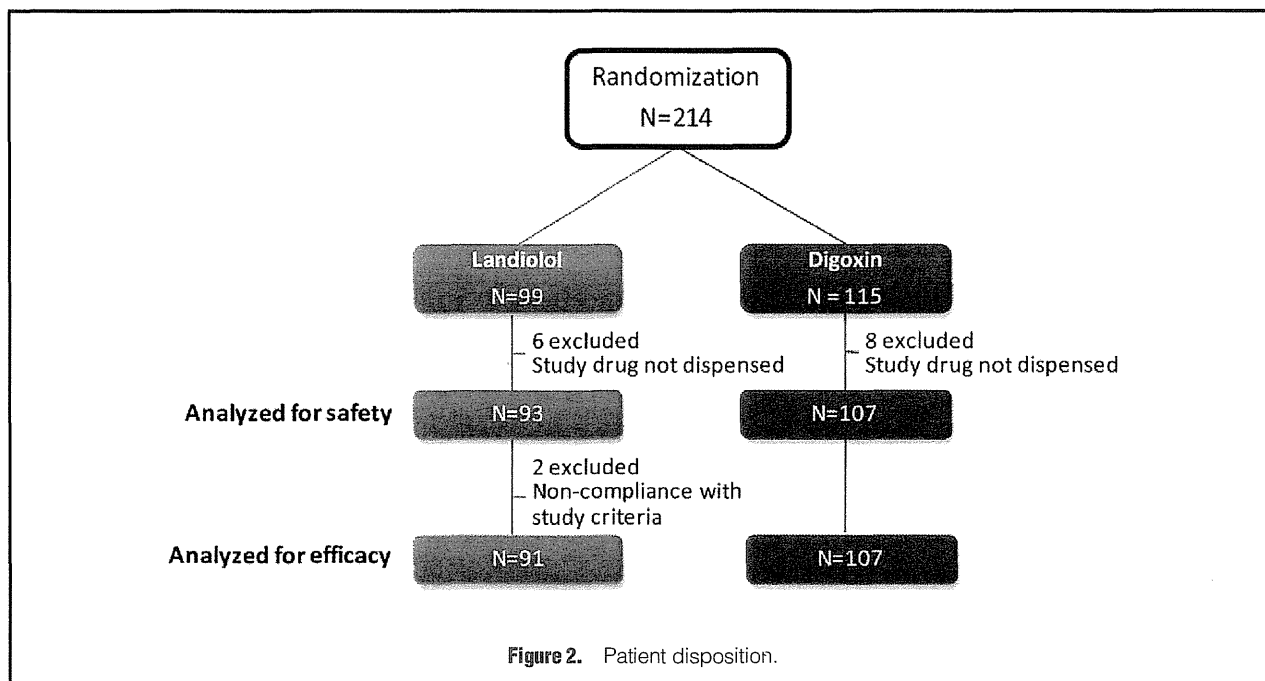
chest pain, dizziness, dyspnea, and edema) at these times.

The safety endpoint was the incidence of adverse events related or unrelated to the study drugs. Adverse events that resulted in death, were life-threatening, required hospitalization or prolonged hospitalization, resulted in persistent or significant disability/incapacity, and crucial medical events were classified as serious adverse events.

After completing the observations at 2h after starting the administration of landiolol, it was replaced with an oral β-blocker, as deemed necessary, at the investigator's discretion.

Statistical Analysis

Data are expressed as the mean±standard deviation or percentages of patients. Student's t-test and X^2 test were used to compare the means and percentages, respectively, between the 2 groups. The primary endpoint was compared between the 2 groups using a linear probability model with HR and LVEF measured immediately before starting the study drug as covariates. The changes in HR and BP after starting the study drugs were compared between the 2 groups using a linear mixed-effects model with adjustment for HR/BP and LVEF before starting the study drug. The following covariance structures were considered: unstructured, compound symmetrical, first-order autoregressive, and Toeplitz. The covariance structure that provided the best fit according to the Akaike information criterion was used in the analysis. Assessment times were treated as categorical factors. Student's t-test was used to compare outcomes between the 2 groups at each time, while the paired t-test was used to compare values between baseline and each time within each group. Bonferroni correction was used for multiple comparisons, except for the change in BP, which was assessed as a safety parameter. Subjective symptoms and objective findings (palpitations, chest pain, dizziness, dyspnea, and edema) were analyzed using the Wilcoxon rank sum test for comparisons between the 2 groups and the Wilcoxon signed rank sum test for comparisons within each

group. Values of P<0.05 were considered statistically significant (2-sided). All analyses were performed using SAS version 9.2 for Windows (SAS Institute, Cary, NC, USA).

Results

Patient Disposition and Baseline Characteristics

The disposition of patients in this study is shown in Figure 2. A total of 214 patients were randomized to either landiolol (n=99) or digoxin (n=115). Of these, 14 patients were not treated (landiolol group, n=6; digoxin group, n=8) and 2 patients in the landiolol group did not comply with the protocol. Therefore, 200 patients (landiolol, n=93; digoxin, n=107) were included in the safety analysis set and 198 patients were included in the efficacy analysis set (landiolol group, n=91; digoxin group, n=107).

The demographics of the study patients are shown in Table 1. There were no differences in the general characteristics of the 2 groups. The mean age was 71.6±11.5 years, and 106 patients (53.0%) were male. The type of atrial tachyarrhythmia at entry was AF in 174 patients (87.0%), AFL in 21 patients (10.5%), and a mixture of AF/AFL in 4 patients (2.0%). The cardiovascular disease was hypertension in 133 patients (66.5%), ischemic heart disease in 30 patients (15.0%), and cardiomyopathy in 13 patients (6.5%). The mean HR was 138.1±15.3 beats/min and the mean LVEF was 36.6±7.6%. The NYHA class was III in 163 patients (81.9%) and IV in 36 patients (18.1%). Before starting study treatment, diuretics were used in 100 patients (50.0%), oral β-blockers were used in 41 patients (20.5%), and nitrate was used in 29 patients (14.5%).

Effects of Landiolol on AF and AFL

The changes in HR and BP for 2h after starting the administration of landiolol and digoxin are shown in Figure 3. Landiolol and digoxin significantly decreased the HR from baseline for over 30min after administration. However, the

Table 1. Baseline Characteristics of Patients With Atrial Fibrillation or Flutter and Left Ventricular Dysfunction

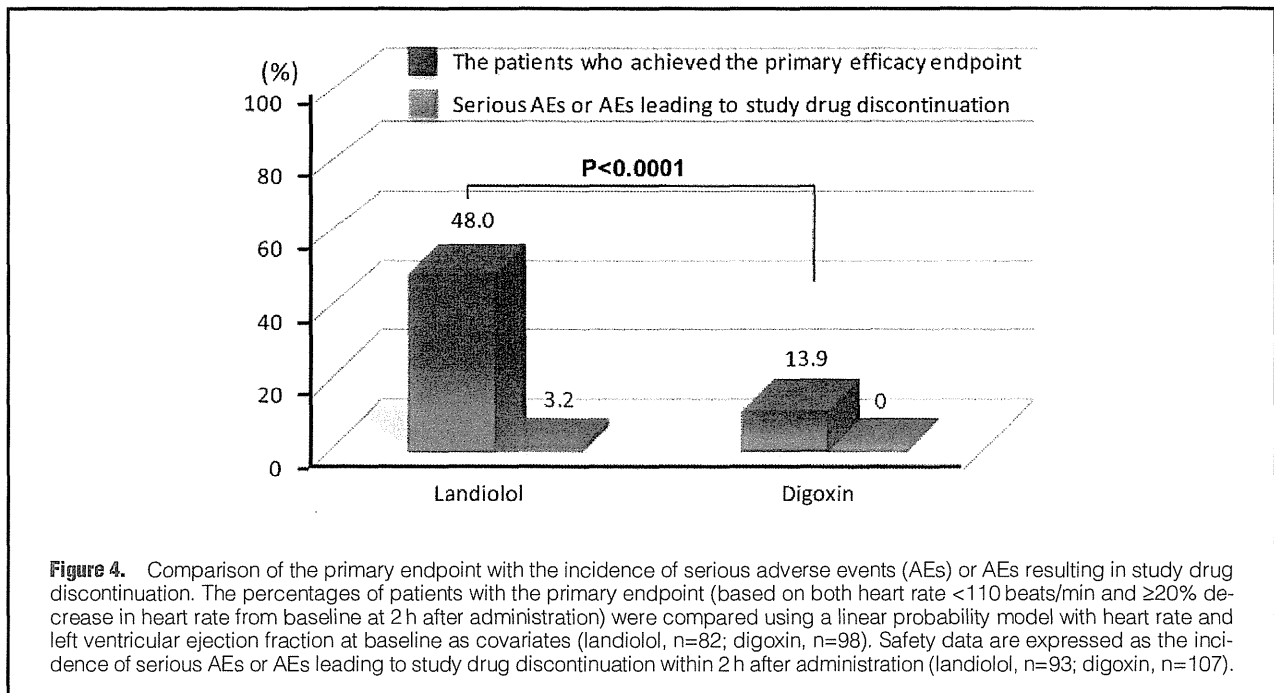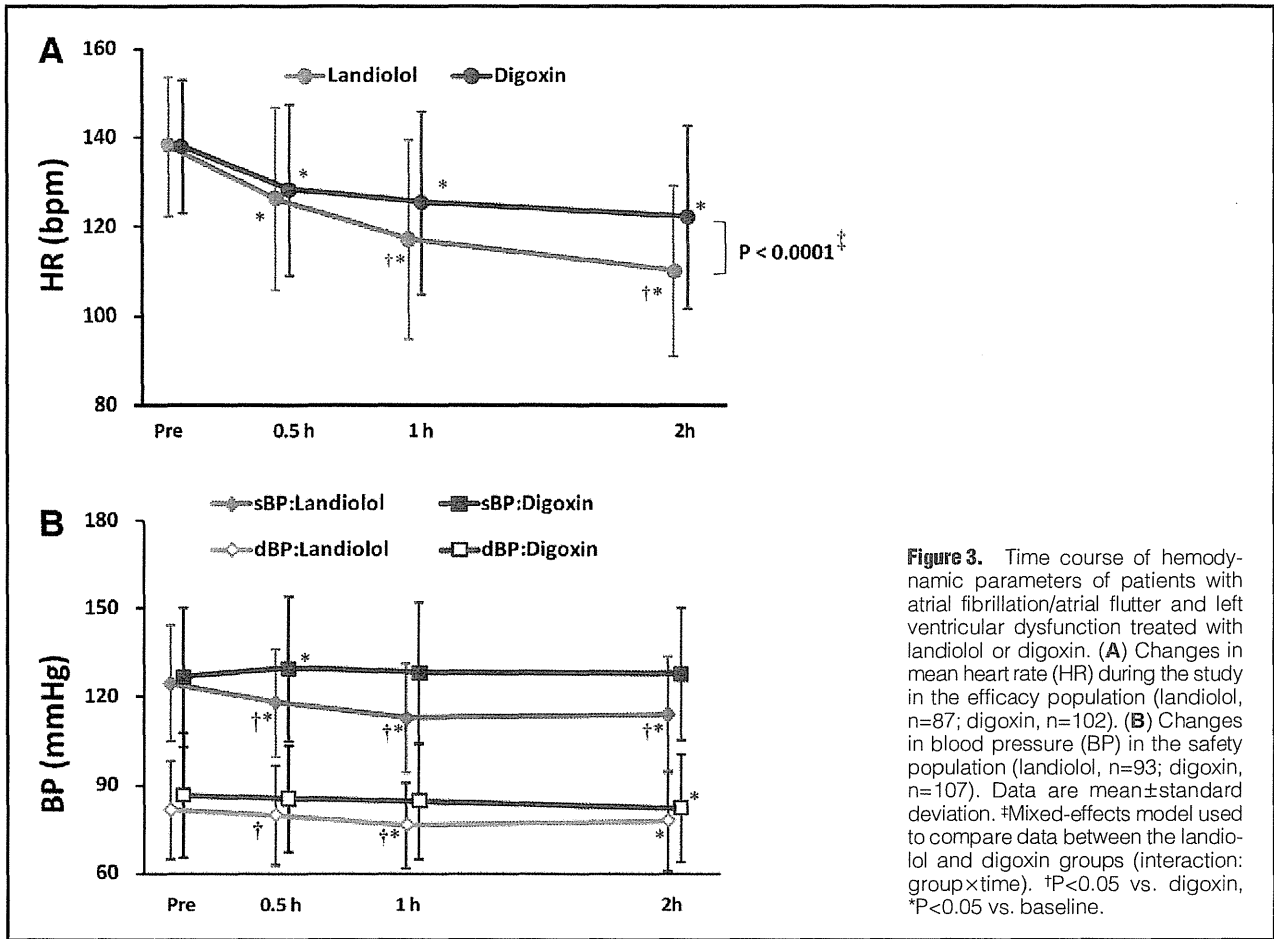|	Total (n=200)	Landiolol (n=93)	Digoxin (n=107)	P value
Demographic characteristics				
Age (years)	71.6±11.5	70.5±12.0	72.5±11.0	0.221
Male, n (%)	106 (53.0)	50 (53.8)	56 (52.3)	0.840
Weight (kg)	60.5±13.2	60.8±13.4	60.2±13.1	0.732
Baseline arrhythmia, n (%)				
Atrial fibrillation	174 (87.0)	80 (86.0)	94 (87.9)	0.095
Atrial flutter	21 (10.5)	8 (8.6)	13 (12.1)	
Atrial fibrillation or flutter	4 (2.0)	4 (4.3)	0 (0)	
Other	1 (0.5)	1 (1.1)	0 (0)	
History of heart failure, n (%)	120 (60.0)	57 (61.3)	63 (58.9)	0.728
Baseline CV disease, n (%)				
Hypertension	133 (66.5)	63 (67.7)	70 (65.4)	0.729
Ischemic heart disease	30 (15.0)	12 (12.9)	18 (16.8)	0.439
DCM	11 (5.5)	6 (6.5)	5 (4.7)	0.582
HCM	2 (1.0)	2 (2.2)	0 (0)	0.127
Hemodynamic parameters				
HR (beats/min)	138.1±15.3	138.2±15.7	138.0±15.0	0.934
SBP (mmHg)	125.7±21.8	124.6±19.8	126.6±23.5	0.523
DBP (mmHg)	84.2±19.2	81.5±16.5	86.5±21.1	0.068
LVEF (%)	36.6±7.6	36.4±7.9	36.7±7.3	0.753
Creatinine (mg/dl)	0.98±0.32	0.98±0.33	0.97±0.32	0.883
BNP (pg/ml)	661.7±561.0	688.0±663.8	639.0±456.6	0.540
NYHA class, n (%)				
III	163 (81.9)	71 (77.2)	92 (86.0)	0.108
IV	36 (18.1)	21 (22.8)	15 (14.0)	
Treatment before administration, n (%)				
Diuretic	100 (50.0)	48 (51.6)	52 (48.6)	0.671
hANP	67 (33.5)	28 (30.1)	39 (36.4)	0.343
β-blocker (oral)	41 (20.5)	18 (19.4)	23 (21.5)	0.708
ARB	31 (15.5)	13 (14.0)	18 (16.8)	0.579
Nitrate	29 (14.5)	11 (11.8)	18 (16.8)	0.317
Aldosterone antagonist	25 (12.5)	11 (11.8)	14 (13.1)	0.789
ACE inhibitor	17 (8.5)	7 (7.5)	10 (9.3)	0.645
Digitalis (oral)	8 (4.0)	6 (6.5)	2 (1.9)	0.099

Data are mean±standard deviation, or n (%).
One patient with PSVT who violated the study protocol was enrolled, but the NYHA class was missing.
ACE, angiotensin-converting enzyme; ARB, angiotensin type 1 receptor blocker; BNP, B-type natriuretic peptide; CV, cardiovascular; DBP, diastolic blood pressure; DCM, dilated cardiomyopathy; hANP, human atrial natriuretic peptide; HCM, hypertrophic cardiomyopathy; HR, heart rate; LVEF, left ventricular ejection fraction; NYHA, New York Heart Association; PSVT, paroxysmal supraventricular tachycardia; SBP, systolic blood pressure.

HR was significantly lower in the landiolol group than in the digoxin group at 1 h (117.3 vs. 125.4 beats/min) and 2 h (110.2 vs. 122.3 beats/min) after starting administration. The magnitude of the reduction in HR was significantly greater in the landiolol group than in the digoxin group (mixed-effects model: group, P=0.0001; time, P<0.0001; interaction [group×time], P<0.0001). The change in HR from baseline to 2 h was −27.0± 13.3 beats/min in the landiolol group and −16.0±13.0 beats/min in the digoxin group. By contrast, the changes in systolic and diastolic BPs over time were not significantly different between the 2 groups (mixed-effects model: group, P<0.0001 and P=0.06; time, P=0.001 and P=0.03; interaction [group×time], P=0.14 and P=0.14, respectively). However, systolic BP was significantly different between the 2 groups at 30 min onward (30 min: 118.1 vs. 129.5 mmHg; 1 h: 112.9 vs. 127.9 mmHg; 2 h: 114.1

vs. 127.7 mmHg). Diastolic BP was also significantly different between the landiolol and digoxin groups at 30 min (79.7 vs. 85.3 mmHg) and 1 h (76.4 vs. 84.5 mmHg).

The results for the primary endpoint are shown in **Figure 4**. The percentage of patients with both a HR <110 beats/min and ≥20% decrease from baseline to 2 h after administration was determined to examine the influence of HR and LVEF at baseline. Overall, 48.0% (n=40/82) of patients in the landiolol group and 13.9% (n=13/98) of patients in the digoxin group achieved the primary endpoint, with a between-group difference of 34.1% (95% confidence interval, 22.1–46.2; P<0.0001). AF/AFL was converted to sinus rhythm within 2 h in 2 patients (2.2%) in the landiolol group and in 2 patients (1.9%) in the digoxin group. The mean dose of landiolol at 2 h was 6.7±3.2 μg·kg⁻¹·min⁻¹. The percentage of patients who achieved the primary endpoint

Figure 3. Time course of hemodynamic parameters of patients with atrial fibrillation/atrial flutter and left ventricular dysfunction treated with landiolol or digoxin. (**A**) Changes in mean heart rate (HR) during the study in the efficacy population (landiolol, n=87; digoxin, n=102). (**B**) Changes in blood pressure (BP) in the safety population (landiolol, n=93; digoxin, n=107). Data are mean±standard deviation. ‡Mixed-effects model used to compare data between the landiolol and digoxin groups (interaction: group×time). †P<0.05 vs. digoxin, *P<0.05 vs. baseline.

Figure 4. Comparison of the primary endpoint with the incidence of serious adverse events (AEs) or AEs resulting in study drug discontinuation. The percentages of patients with the primary endpoint (based on both heart rate <110 beats/min and ≥20% decrease in heart rate from baseline at 2h after administration) were compared using a linear probability model with heart rate and left ventricular ejection fraction at baseline as covariates (landiolol, n=82; digoxin, n=98). Safety data are expressed as the incidence of serious AEs or AEs leading to study drug discontinuation within 2h after administration (landiolol, n=93; digoxin, n=107).
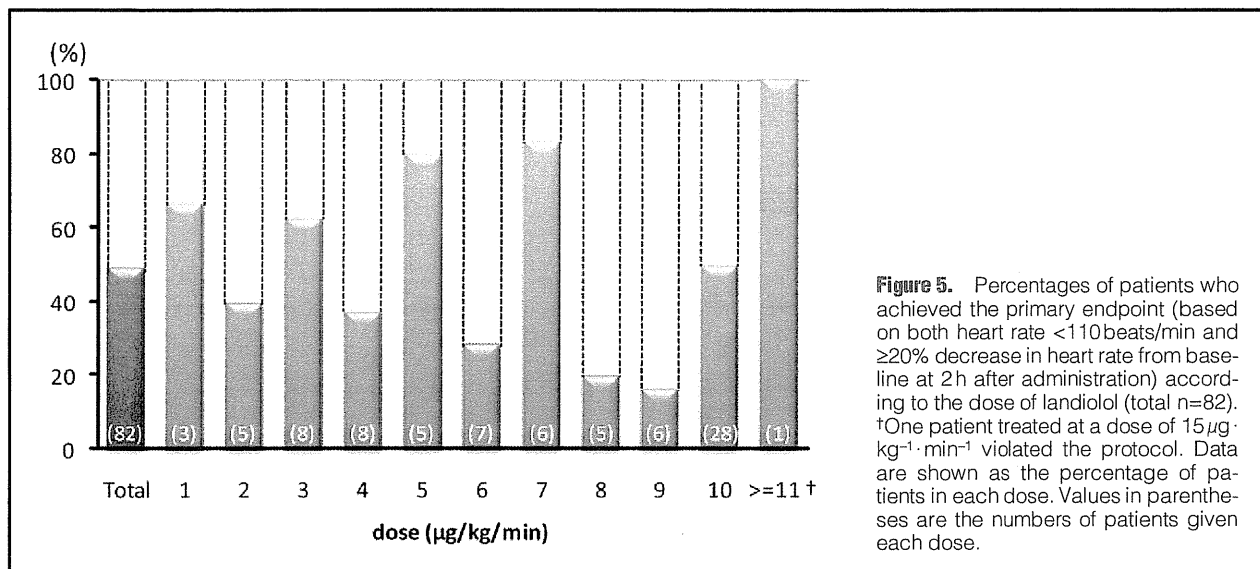
Figure 5. Percentages of patients who achieved the primary endpoint (based on both heart rate <110 beats/min and ≥20% decrease in heart rate from baseline at 2 h after administration) according to the dose of landiolol (total n=82). †One patient treated at a dose of 15 μg · kg⁻¹ · min⁻¹ violated the protocol. Data are shown as the percentage of patients in each dose. Values in parentheses are the numbers of patients given each dose.

Table 2. Incidence of AEs in Patients With Atrial Fibrillation or Flutter and Left Ventricular Dysfunction Treated With Landiolol or Digoxin

	Landiolol (n=93)		Digoxin (n=107)	
	0–2 h	Total	0–2 h	Total
All, n (%)	8 (8.6)	30 (32.2)	2 (1.9)	35 (32.7)
Any serious AE, n (%)	1 (1.1)	2 (2.2)	0 (0)	3 (2.8)
Any AE leading to study drug discontinuation, n (%)	3 (3.2)	3 (3.2)	0 (0)	0 (0)
AEs occurring in >3%, n (%)				
Hypotension	3 (3.2)	7 (7.5)	0 (0)	4 (3.7)
Vomiting	0 (0)	4 (4.3)	0 (0)	1 (0.9)
Nausea	0 (0)	3 (3.2)	0 (0)	0 (0)
Increased creatinine*	0 (0)	3 (3.2)	0 (0)	3 (2.8)
Increased urea*	0 (0)	3 (3.2)	0 (0)	1 (0.9)
Constipation	0 (0)	0 (0)	0 (0)	4 (3.7)

Data are n (%). "0–2 h" included the number of patients with events occurring within 2 h after starting treatment. "Total" included the number of patients with events occurring between the start of treatment and the final observation. Only AEs occurring at a frequency of ≥3% are shown.
*Defined as an increase in values from normal to abnormal or worsening of the parameter from baseline; these events were judged by the investigators as an AE based on the clinical significance of the change. AEs, adverse events.

Table 3. Changes in Parameters at the Final Observation in Patients With Atrial Fibrillation or Flutter and Left Ventricular Dysfunction Treated With Landiolol or Digoxin

	Landiolol (n=93)		Digoxin (n=107)	
	Pre	Final	Pre	Final
HR (beats/min)	138.2±15.7	98.3±17.6	138.0±15.0	102.3±19.8
SBP (mmHg)	124.6±19.8	113.3±18.4	126.6±23.5	115.5±18.0
DBP (mmHg)	81.5±16.5	72.8±14.3	86.5±21.1	72.1±15.1
LVEF (%)	36.4±7.9	43.1±13.1	36.7±7.3	44.2±11.0
Creatinine (mg/dl)	0.98±0.33	0.99±0.35	0.97±0.32	0.94±0.31
NYHA class, n (%)				
None		0 (0)		1 (0.9)
I		12 (13.6)		12 (11.3)
II		50 (56.8)		51 (48.1)
III	71 (77.2)	24 (27.3)	92 (86.0)	40 (37.7)
IV	21 (22.8)	2 (2.3)	15 (14.0)	2 (1.9)

The final observation was performed at 48 h after the end of administration of landiolol or at 48 h after the final dose in the digoxin group. Abbreviations as in Table 1.

in the landiolol group at each dose is shown in Figure 5. The effective dose of landiolol ranged from 1 to $10\,\mu g \cdot kg^{-1} \cdot min^{-1}$ without dose-dependency.

The changes in subjective symptoms and objective findings (palpitations, chest pain, dizziness, dyspnea, and edema) during the study treatment are shown in Table S1. Palpitations, dyspnea, and edema improved significantly from baseline to 2h in both groups. However, there were no clinically relevant differences in subjective symptoms or objective findings between the 2 groups. The mean duration of treatment with landiolol was 20.4 ± 20.8h (range, 0.8–72h), and the mean dose of landiolol throughout the treatment was $6.3 \pm 3.5\,\mu g \cdot kg^{-1} \cdot min^{-1}$. After the study treatment period, landiolol was replaced bisoprolol in 47 patients (50.5%) and by carvedilol in 27 patients (29.0%), at maintenance doses of 1.8 ± 1.3mg and 3.2 ± 2.7mg, respectively.

Safety

The incidence of adverse events is shown in Table 2. Adverse events occurred in 30 patients (32.3%) in the landiolol group and in 35 patients (32.7%) in the digoxin group, which was not statistically significant (P=0.95). During the 2-h treatment period, adverse events occurred in 8 patients (8.6%) in the landiolol group and in 2 patients (1.9%) in the digoxin group, which was statistically significant (P=0.029). Hypotension was reported as an adverse event in 7 patients (7.5%) in the landiolol group and in 4 patients (3.7%) in the digoxin group, showing no significant difference between the 2 groups (P=0.24). Vomiting and nausea were reported in 4 patients (4.3%) and 3 patients (3.2%), respectively, in the landiolol group. Vomiting was reported in 1 patient (0.9%) in the digoxin group, but nausea was not reported in this group.

Serious adverse events were reported in 2 patients in the landiolol group (congestive heart failure and embolic stroke in 1 patient each) and in 3 patients in the digoxin group (sinus arrest, diabetes insipidus, and pneumonia in 1 patient each). One patient in the landiolol group developed acute exacerbation of congestive heart failure at 12h after the end of administration of landiolol. Despite the intensive treatments, the patient died at 31h after the end of administration of landiolol. The administration of landiolol was stopped in 3 patients because of an adverse event (embolic stroke, hypotension, and asthma in 1 patient each).

The changes in the hemodynamic parameters, renal function, and symptoms at the final observation are shown in Table 3. The period to the final observation was 66.6 ± 22.5h in the landiolol group and 49.9 ± 11.9h in the digoxin group. None of the laboratory parameters worsened from baseline to the end of the study in either group. The brain natriuretic peptide levels did not increase from baseline in either group (Figure S1).

Discussion

The results of this study show that continuous intravenous administration of landiolol in a dose-escalating manner effectively controlled rapid HR in patients with AF/AFL and LV dysfunction. Landiolol and digoxin were effective in 48.0% and 13.9% of patients, respectively, at 2h after starting treatment, indicating that the ultra-short-acting landiolol is more useful than the slow-acting digoxin. Regarding the safety of these drugs for rapid control of HR, the incidence of hypotension was similar in both groups. During treatment with landiolol, which rapidly reaches steady state and has a half-life of 4min, the risk of hypotension may be low because its dose can

be carefully adjusted according to the patient's condition. Other adverse effects associated with a reduction in HR include gastrointestinal symptoms such as nausea/vomiting caused by blood flow stasis. However, there were no abnormal changes in laboratory data, including serum bilirubin levels.

It has been reported that the control of HR in patients with tachycardic AF/AFL helps to prevent worsening of heart failure and ventricular dysfunction, because it contributes to improvements in circulatory dynamics and subjective symptoms.[16-18] However, the optimal target HR in the treatment of AF/AFL in patients with LV dysfunction has not been clearly established. In patients with LV dysfunction, a rapid and vigorous decrease in HR might be detrimental if accompanied by a decrease in cardiac output. However, in the RACE II study, which was conducted in patients with persistent AF and normal to moderate LV dysfunction, there were no differences in prognosis, including mortality, incidence of heart failure, and improvements in subjective symptoms, between the lenient control (resting HR <110 beats/min) and strict control (resting HR <80 beats/min and HR during moderate exercise <110 beats/min) groups.[19] In the present study conducted in patients with LV dysfunction and NYHA class III or IV symptoms, the target HR of <110 beats/min, corresponding to the lenient criterion in the RACE II study, may be reasonable based on the results of earlier studies. In addition, a 20% decrease in HR from baseline has been conventionally used to verify the drug-induced HR reduction in AF.[20,21] Accordingly, the primary endpoint in this study combined both criteria.

In general, the optimal dose of β-blockers in patients with LV dysfunction should be determined according to the patient's cardiac function and general condition. It should also be noted that the response to β-blockers in patients with AF varies depending on polymorphisms (eg, G389R and S49G) in the $\beta 1$ receptor gene.[22] In fact, the present study showed that the optimal dose varied among the patients with variable response to landiolol. Therefore, the optimal dose of β-blocker for HR control cannot be determined before treatment. The dosage of rate-controlling drugs for treating AF/AFL in patients with LV dysfunction should be highly adjustable, according to the patient's hemodynamic response. The efficacy and safety results of this study provide support for the ultra-fast-acting and easily adjustable landiolol for swift control of rapid HR in patients with AF/AFL and LV dysfunction. However, in the present study, there were no significant differences between the 2 groups in the subjective symptoms reported within 2h after starting administration. The rapid decrease in HR elicited by landiolol may not necessarily be associated with symptomatic relief in these patients. These findings suggest that it is difficult to evaluate how rapid HR contributes to the hemodynamic status and symptoms of heart failure in patients with AF/AFL.

The guidelines of the American Heart Association and the European Society of Cardiology recommend digitalis and amiodarone for acute rate-control therapy in patients with AF and LV dysfunction.[9,23,24] Although amiodarone is classified as a rhythm-control drug, it can also decrease the HR because it blocks K^+ channels, Ca^{2+} channels, and β receptors. However, because amiodarone has a long half-life, it is difficult to adjust its dose according to the patient's condition.

In the present study, we observed better control of HR with landiolol than with digoxin. As landiolol was the only intravenous β-blocker used in this study, the efficacy of esmolol, propranolol, and amiodarone in this setting remains unknown. Thus, we cannot confirm whether landiolol is more effective than these drugs. Nevertheless, landiolol may be easier to use

than other drugs for acute rate-control therapy in patients with AF/AFL and LV dysfunction because it is faster-acting and shows greater selectivity for β1 receptors than esmolol, propranolol or amiodarone. In addition, this study was intended to test the usefulness of landiolol in acute rate-control therapy with up to 5 days of follow-up. Therefore, the medium- and long-term prognosis of these patients after treatment with landiolol should be studied in future.

Conclusions

In the treatment of AF/AFL in patients with LV dysfunction, landiolol rapidly decreased the HR in approximately 50% of the patients, and was more effective for urgent HR control than digoxin, without an increase in the incidence of adverse events. Landiolol is an ultra-short-acting, highly cardioselective intravenous β-blocker that could be a promising drug for controlling rapid HR in patients with AF/AFL and LV dysfunction.

References

1. Hamaguchi S, Yokoshiki H, Kinugawa S, Tsuchihashi-Makaya M, Yokota T, Takeshita A, et al; JCARE-CARD Investigators. Effects of atrial fibrillation on long-term outcomes in patients hospitalized for heart failure in Japan: A report from the Japanese Cardiac Registry of Heart Failure in Cardiology (JCARE-CARD). Circ J 2009; 73: 2084–2090.
2. Maisel WH, Stevenson LW. Atrial fibrillation in heart failure: Epidemiology, pathophysiology, and rationale for therapy. Am J Cardiol 2003; 91: 2D–8D.
3. Sato N, Kajimoto K, Asai K, Mizuno M, Minami Y, Nagashima M, et al. Acute decompensated heart failure syndromes (ATTEND) registry: A prospective observational multicenter cohort study: Rationale, design, and preliminary data. Am Heart J 2010; 159: 949–955.
4. JCS Joint Working Group. Guidelines for pharmacotherapy of atrial fibrillation (JCS 2008): Digest version. Circ J 2010; 74: 2479–2500.
5. Clark DM, Plumb VJ, Epstein AE, Kay GN. Hemodynamic effects of an irregular sequence of ventricular cycle lengths during atrial fibrillation. J Am Coll Cardiol 1997; 30: 1039–1045.
6. Wang TJ, Larson MG, Levy D, Vasan RS, Leip EP, Wolf PA, et al. Temporal relations of atrial fibrillation and congestive heart failure and their joint influence on mortality: The Framingham Heart Study. Circulation 2003; 107: 2920–2925.
7. Peters KG, Kienzle MG. Severe cardiomyopathy due to chronic rapidly conducted atrial fibrillation: Complete recovery after restoration of sinus rhythm. Am J Med 1988; 85: 242–244.
8. Grogan M, Smith HC, Gersh BJ, Wood DL. Left ventricular dysfunction due to atrial fibrillation in patients initially believed to have idiopathic dilated cardiomyopathy. Am J Cardiol 1992; 69: 1570–1573.
9. Fuster V, Rydén LE, Cannom DS, Crijns HJ, Curtis AB, Ellenbogen KA, et al. 2011 ACCF/AHA/HRS focused updates incorporated into the ACC/AHA/ESC 2006 Guidelines for the management of patients with atrial fibrillation: A report of the American College of Cardiology Foundation/American Heart Association Task Force on Practice Guidelines developed in partnership with the European Society of Cardiology and in collaboration with the European Heart Rhythm Association and the Heart Rhythm Society. J Am Coll Cardiol 2011; 57: e101–e198.
10. The Digitalis in Acute Atrial Fibrillation (DAAF) Trial Group. Intravenous digoxin in acute atrial fibrillation: Results of a randomized, placebo-controlled multicentre trial in 239 patients: The Digitalis in Acute Atrial Fibrillation (DAAF) Trial Group. Eur Heart J 1997; 18:

649–654.
11. Shiroya T, Ichioka Y, Yoshida K, Nishijima K, Omawari N, Naka M, et al. Pharmacological studies of ONO-1101 as a beta-blocking agent with high beta 1 selectivity and ultra-short duration of action. Kiso To Rinsho 1997; 31: 2913–2923 (in Japanese).
12. Sakamoto A, Kitakaze M, Takamoto S, Namiki A, Kasanuki H, Hosoda S; JL-KNIGHT study group. Landiolol, an ultra-short-acting β1-blocker, more effectively terminates atrial fibrillation than diltiazem after open heart surgery: Prospective, multicenter, randomized, open-label study (JL-KNIGHT study). Circ J 2012; 76: 1097–1101.
13. Hanada K, Higuma T, Nishizaki F, Sukekawa T, Yokota T, Yamada M, et al. Randomized study on the efficacy and safety of landiolol, an ultra-short-acting β1-adrenergic blocker, in patients with acute myocardial infarction undergoing primary percutaneous coronary intervention. Circ J 2012; 76: 439–445.
14. Kobayashi S, Susa T, Tanaka T, Murakami W, Fukuta S, Okuda S, et al. Low-dose β-blocker in combination with milrinone safely improves cardiac function and eliminates pulsus alternans in patients with acute decompensated heart failure. Circ J 2012; 76: 1646–1653.
15. Miwa Y, Ikeda T, Mera H, Miyakoshi M, Hoshida K, Yanagisawa R, et al. Effects of landiolol, an ultra-short-acting β1-selective blocker, on electrical storm refractory to class III antiarrhythmic drugs. Circ J 2010; 74: 856–863.
16. Pinter A, Dorian P, Paquette M, Ng A, Burns M, Spanu I, et al. Left ventricular performance during acute rate control in atrial fibrillation: The importance of heart rate and agent used. J Cardiovasc Pharmacol Ther 2003; 8: 17–24.
17. Lip GY, Tse HF. Management of atrial fibrillation. Lancet 2007; 370: 604–618.
18. Siu CW, Lau CP, Lee WL, Lam KF, Tse HF. Intravenous diltiazem is superior to intravenous amiodarone or digoxin for achieving ventricular rate control in patients with acute uncomplicated atrial fibrillation. Crit Care Med 2009; 37: 2174–2179.
19. Van Gelder IC, Groenveld HF, Crijns HJ, Tuininga YS, Tijssen JG, Alings AM, et al; RACE II Investigators. Lenient versus strict rate control in patients with atrial fibrillation. N Engl J Med 2010; 362: 1363–1373.
20. Gray RJ, Bateman TM, Czer LS, Conklin CM, Matloff JM. Esmolol: A new ultrashort-acting beta-adrenergic blocking agent for rapid control of heart rate in postoperative supraventricular tachyarrhythmias. J Am Coll Cardiol 1985; 5: 1451–1456.
21. Dias VC, Weir SJ, Ellenbogen KA. Pharmacokinetics and pharmacodynamics of intravenous diltiazem in patients with atrial fibrillation or atrial flutter. Circulation 1992; 86: 1421–1428.
22. Parvez B, Chopra N, Rowan S, Vaglio JC, Muhammad R, Roden DM, et al. A common β1-adrenergic receptor polymorphism predicts favorable response to rate-control therapy in atrial fibrillation. J Am Coll Cardiol 2012; 59: 49–56.
23. European Heart Rhythm Association; European Association for Cardio-Thoracic Surgery, Camm AJ, Kirchhof P, Lip GY, Schotten U, et al. Guidelines for the management of atrial fibrillation: The Task Force for the Management of Atrial Fibrillation of the European Society of Cardiology (ESC). Eur Heart J 2010; 31: 2369–2429.
24. Hofmann R, Steinwender C, Kammler J, Kypta A, Wimmer G, Leisch F. Intravenous amiodarone bolus for treatment of atrial fibrillation in patients with advanced congestive heart failure or cardiogenic shock. Wien Klin Wochenschr 2004; 116: 744–749.

Appendix

Investigators and Study Sites

Toshiharu Takeuchi, Asahikawa Medical University Hospital; Shigeo Kakinoki, Otaru Kyokai Hospital; Minoru Sato, Hokkaido Medical Center; Hironori Murakami, Teine Keijinkai Hospital; Ken Okumura, Hirosaki University Graduate School of Medicine; Tetsuo Yagi, Sendai City Hospital; Tsuyoshi Shinozaki, Sendai Medical Center; Koji Fukuda, Tohoku University Graduate School of Medicine; Kaname Takizawa, Sendai Kousei Hospital; Tetsu Watanabe, Yamagata University Hospital; Shuichi Taguchi, Mito Medical Center; Shoji Suzuki, Kasumigaura Medical Center; Kazutaka Aonuma, Tsukuba University Hospital; Daisuke Abe, Ibaraki Prefectural Central Hospital; Shoichi Tange, Maebashi Red Cross Hospital; Shigeto Naito, Gunma Prefectural Cardiovascular Center; Shu Kasama, Cardiovascular Hospital of Central Japan (Kitakanto Cardiovascular Hospital); Shin-ichi Momomura, Saitama Medical Center, Jichi Medical University; Kazuo Matsumoto, Saitama Medical University International Medical Center; Masayuki Inagaki, Funabashi Municipal Medical Center; Atsushi Iwasa, New Tokyo Hospital; Yoshihiko Seino, Nippon Medical School Chiba-Hokusoh Hospital; Atsushi Hirayama, Nihon University School of Medicine, Itabashi Hospital; Takanori Ikeda, Toho University Omori Medical Center; Seiji Fukamizu, Tokyo

−128−

Metropolitan Hiroo Hospital; Jun Umemura, Sakakibara Heart Institute; Hiroyuki Niinuma, St. Luke's International Hospital; Koichiro Kinugawa, Tokyo University Hospital; Kaoru Sugi, Toho University Ohashi Medical Center; Hiroyuki Tanaka, Tokyo Metropolitan Tama Medical Center; Yoshiki Kusama, Nippon Medical School Tama-Nagayama Hospital; Atsuyuki Ono, Kasai Shoikai Hospital; Takeshi Yamashita, The Cardiovascular Institute; Kazunori Iwade, National Hospital Organization Yokohama Medical Center; Kazuo Kimura, Yokohama City University Medical Center; Hiroshi Suzuki, Showa University Fujigaoka Hospital; Hideo Himeno, Fujisawa City Hospital; Koichiro Yoshioka, Tokai University Hospital; Hiroshi Furushima, Niigata University Graduate School of Medical and Dental Sciences; Hirotaka Oda, Niigata City General Hospital; Koichi Fuse, Tachikawa General Hospital; Hiroshi Inoue, Toyama University Hospital; Tetsuo Konno, Kanazawa University Hospital; Masayuki Takamura, Kanazawa University Hospital; Kenji Sakata, Kanazawa Cardiovascular Hospital; Ken Umetani, Yamanashi Prefectural Central Hospital; Kenichi Kawabata, Yamanashi University Hospital; Hiroshi Tsutsui, Japanese Red Cross Society Suwa Hospital; Masahiro Muto, Hamamatsu Medical Center; Yasushi Wakabayashi, Seirei Mikatahara General Hospital; Yasuya Inden, Nagoya University Hospital; Hiroaki Sano, Nagoya Ekisaikai Hospital; Haruo Kamiya, Japanese Red Cross Nagoya Daiichi Hospital; Toshikazu Tanaka, Okazaki City Hospital; Masayoshi Ajioka, Tosei General Hospital; Yukio Ozaki, Fujita Health University Hospital; Tetsuya Amano, Aichi Medical University Hospital; Makoto Kitamuta, Kyoto Second Red Cross Hospital; Masahiro Esato, Ijinkai Takeda General Hospital; Kimihito Usui, Maizuru Mutual Hospital; Eiwa Zen, Koseikai Takeda Hospital; Kenshi Fujii, Sakurabashi Watanabe Hospital; Takahisa Yamada, Osaka General Medical Center; Yasushi Sakata, Osaka University Hospital; Yoshiyuki Nagai, Rinku General Medical Center; Shiro Kamakura, National Cerebral and Cardiovascular Center; Takashi Kurita, Kinki University Hospital; Akihiko Takahashi, Sakurakai Takahashi Hospital; Toshiro Shinke, Kobe University Hospital; Kazuyasu Yoshitani, Hyogo Prefectural Amagasaki Hospital; Takatoshi Hayashi, Hyogo Brain and Heart Center; Yorihiko Higashino, Higashi Takarazuka Satoh Hospital; Koichi Tamita, Nishinomiya Watanabe

Cardiovascular Center; Satoshi Nagase, Okayama University Hospital; Ritsu Tamura, National Hospital Organization Kure Medical Center; Kaoru Yanagihara, Higashihiroshima Medical Center; Nobuo Shiode, Tsuchiya General Hospital; Yuji Shimatani, Hiroshima City Hospital; Mitsunori Okamoto, Hiroshima Prefectural Hospital; Shigeki Kobayashi, Yamaguchi University Hospital; Shinobu Hosokawa, Tokushima Red Cross Hospital; Eitaro Umehara, Kaisei Hospital; Mitsunori Abe, Yotsuba Circulation Clinic; Masahiko Goya, Kokura Memorial Hospital; Toshiaki Kadokami, Saiseikai Futsukaichi Hospital; Yusuke Yamamoto, Saiseikai Fukuoka General Hospital; Keijiro Saku, Fukuoka University Hospital; Ryozo Kobayashi, National Hospital Organization Kyusyu Medical Center; Tomohiro Kawasaki, Shin-Koga Hospital; Hiroshige Yamabe, Kumamoto University Hospital; Kazuhiro Nishigami, Saiseikai Kumamoto Hospital Cardiovascular Center; Shunichi Koide, Yatsushiro Social Insurance General Hospital; Masayuki Kaneko, Oita Oka Hospital; Masahiro Sonoda, National Hospital Organization Kagoshima Medical Center; Tetsuji Shinjyo, Tomishiro Central Hospital.

Ono Pharmaceutical Core Team
Takashi Tanaka, Takuto Kuramoto, Taketo Anze, Nobuyuki Oki (data manager), Akira Tsuchiya (data manager), Keita Nagasawa (data manager), Haruka Okamoto (data manager) and Toshihiro Yoshikawa (statistician).

Supplementary Files

Supplementary File 1

Table S1.   Subjective Symptoms and Objective Findings in Patients With Atrial Fibrillation or Flutter and Left Ventricular Dysfunction Treated With Landiolol or Digoxin

Figure S1.   Distribution of levels of B-type natriuretic peptide (BNP).

Please find supplementary file(s);
http://dx.doi.org/10.1253/circj.CJ-12-1618

Induction of human cardiomyocyte-like cells from fibroblasts by defined factors

Rie Wada[a], Naoto Muraoka[a,b], Kohei Inagawa[a,b], Hiroyuki Yamakawa[a,b], Kazutaka Miyamoto[a,b], Taketaro Sadahiro[a,b], Tomohiko Umei[a], Ruri Kaneda[a,b], Tomoyuki Suzuki[b,c], Kaichiro Kamiya[c], Shugo Tohyama[b], Shinsuke Yuasa[b], Kiyokazu Kokaji[d], Ryo Aeba[d], Ryohei Yozu[d], Hiroyuki Yamagishi[e], Toshio Kitamura[f], Keiichi Fukuda[b], and Masaki Ieda[a,b,g,1]

[a]Department of Clinical and Molecular Cardiovascular Research and [b]Department of Cardiology, School of Medicine, Keio University, Tokyo 160-8582, Japan; [c]Department of Cardiovascular Research, Research Institute of Environmental Medicine, Nagoya University, Nagoya 464-8601, Japan; [d]Division of Cardiovascular Surgery and [e]Department of Pediatrics, School of Medicine, Keio University, Tokyo 160-8582, Japan; [f]Division of Cellular Therapy, Institute of Medical Science, University of Tokyo, Tokyo 108-8639, Japan; and [g]Japan Science and Technology Agency CREST, Tokyo 160-8582, Japan

Heart disease remains a leading cause of death worldwide. Owing to the limited regenerative capacity of heart tissue, cardiac regenerative therapy has emerged as an attractive approach. Direct reprogramming of human cardiac fibroblasts (HCFs) into cardiomyocytes may hold great potential for this purpose. We reported previously that induced cardiomyocyte-like cells (iCMs) can be directly generated from mouse cardiac fibroblasts in vitro and vivo by transduction of three transcription factors: Gata4, Mef2c, and Tbx5, collectively termed GMT. In the present study, we sought to determine whether human fibroblasts also could be converted to iCMs by defined factors. Our initial finding that GMT was not sufficient for cardiac induction in HCFs prompted us to screen for additional factors to promote cardiac reprogramming by analyzing multiple cardiac-specific gene induction with quantitative RT-PCR. The addition of Mesp1 and Myocd to GMT up-regulated a broader spectrum of cardiac genes in HCFs more efficiently compared with GMT alone. The HCFs and human dermal fibroblasts transduced with GMT, Mesp1, and Myocd (GMTMM) changed the cell morphology from a spindle shape to a rod-like or polygonal shape, expressed multiple cardiac-specific proteins, increased a broad range of cardiac genes and concomitantly suppressed fibroblast genes, and exhibited spontaneous Ca^{2+} oscillations. Moreover, the cells matured to exhibit action potentials and contract synchronously in coculture with murine cardiomyocytes. A 5-ethynyl-2′-deoxyuridine assay revealed that the iCMs thus generated do not pass through a mitotic cell state. These findings demonstrate that human fibroblasts can be directly converted to iCMs by defined factors, which may facilitate future applications in regenerative medicine.

cell fate conversion | regeneration | cardiogenesis

Cardiovascular disease remains a leading cause of death worldwide, for which current therapeutic regimens remain limited. Given that adult human hearts have little regenerative capacity after injury, the demand is high for cardiac regenerative therapy. The recent discovery of induced pluripotent stem cells (iPSCs) allows the direct generation of specific cell types from differentiated somatic cells by overexpression of lineage-specific factors.

Several previous studies have demonstrated that such direct lineage reprogramming can yield a diverse range of cell types, including pancreatic β cells, neurons, neural progenitors, blood progenitors, and hepatocyte-like cells (1–5). We previously reported that a minimum mixture of three cardiac-specific transcription factors—Gata4, Mef2c, and Tbx5 (GMT)—directly induced cardiomyocyte-like cells (iCMs) from mouse fibroblasts in vitro (6). Following our report, three other groups also reported generation of functional cardiomyocytes from mouse fibroblasts with various combinations of transcription factors, either with GMT plus Hand2 (GHMT) or Mef2c, Myocd, and Tbx5 or using

microRNAs (7–9). Although full reprogramming into beating cardiomyocytes was not efficient in vitro (10, 11), gene transfer of GMT or GHMT into mouse hearts generated new cardiomyocytes from endogenous cardiac fibroblasts and improved cardiac function after myocardial infarction (7, 12, 13). The foregoing studies suggest that direct cardiac reprogramming may be a useful therapeutic approach for regenerative purposes, and that identification of reprogramming factors in human cells is important for the development of this technology (14–16).

In the present study, we sought to generate cardiomyocytes directly from postnatal human fibroblasts. We found that GMT was not sufficient for cardiac reprogramming in human cells. We then screened additional reprogramming factors for their ability to induce cardiac reprogramming by analyzing multiple cardiac gene induction, and found that the addition of Mesp1 and Myocd to GMT was able to generate cardiomyocyte-like cells from human fibroblasts in vitro.

Results

Gata4, Mef2c, Tbx5, Mesp1, and Myocd Induce Multiple Cardiac Gene Expression in Human Cardiac Fibroblasts. We first developed a culture system for human cardiac fibroblasts (HCFs) following our mouse cardiac fibroblast isolation protocol. Human atrial tissues were obtained from 36 patients (age 1 mo to 80 y; average age, 35 y) undergoing cardiac surgery with informed consent following the guidelines of the Keio University Ethics Committee. The $Thy1^+/CD31^-$ FACS-sorted fibroblasts did not express cardiomyocyte or cardiac progenitor cell (CPC) genes, but did express fibroblast genes on quantitative RT-PCR (qRT-PCR) analysis (Fig. S1 A–C). HCFs expressed fibroblast proteins, vimentin, and fibronectin, but not markers of cardiomyocytes, CPCs, smooth muscle cells, or endothelial cells (Fig. 1A and Fig. S1D). The antibody immunoreactivities were confirmed in the positive controls (Fig. S1E). FACS analyses also demonstrated that the HCF population did not contaminate cardiomyocytes (Fig. 1B).

For transduction, we first used the sequential lentivirus/ecotropic retrovirus infection following the iPSC generation protocol from human dermal fibroblasts (HDFs) (17). The transduction efficiency was <20% in HCFs (Fig. 1C). We then directly infected HCFs using other types of retroviruses, produced by PLAT-A cells and PLAT-GP cells (18). We achieved high transduction efficiency
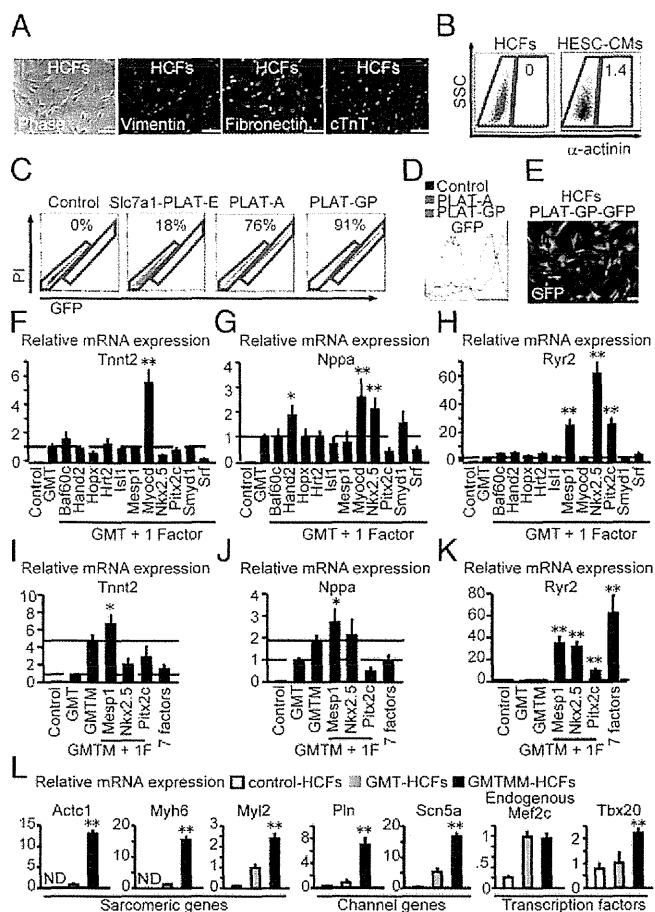
Fig. 1. Gata4, Mef2c, Tbx5, Mesp1, and Myocd induce cardiac gene expression in HCFs. (A) Morphology and characterization of HCFs by phase-contrast imaging, with vimentin, fibronectin, and cTnT immunostaining [passage number 1 (P1) HCFs, 57-y-old patient; $n = 3$]. The antibody immunoreactivities were confirmed in HESC-CMs (Fig. S1E). (B) FACS analysis for α-actinin$^+$ cells (HESC-CMs as a positive control) showed no expression in HCFs (P1 HCFs, 58-y-old patient; $n = 3$). (C) FACS analysis of the HCFs transduced by sequential infection of Slc7a1 lentivirus and ecotropic GFP retrovirus (Slc7a1-PLAT-E), amphotropic GFP retrovirus produced by PLAT-A cells (PLAT-A), and pantropic GFP retrovirus produced by PLAT-GP cells (PLAT-GP) (P1 HCFs from patients aged 1 mo and 50 y; $n = 4$). (D) Histogram of GFP intensity in the transduced HCFs determined by FACS analysis (P1 HCFs from 50-y-old patient; $n = 3$). GFP expression was high in cells transduced with retrovirus produced by PLAT-GP. (E) Image of HCFs infected by the GFP retrovirus produced by PLAT-GP. (F–H) mRNA expression of cardiac genes (Tnnt2, Nppa, and Ryr2) in HCFs transduced with GMT plus individual factors as determined by qRT-PCR after 1 wk of transduction (P1 HCFs, 71-y-old patient; $n = 3$). Data were normalized against the GMT values. See also Fig. S2 A–E and Movie S1. (I–K) The mRNA expression of cardiac genes in HCFs transduced with GMTM plus Mesp1, Nkx2.5, Pitx2c, or all three genes was determined by qRT-PCR after 1 wk of transduction (P1 HCFs, 59-y-old patient; $n = 3$). Data were normalized against the GMT values. (L) Multiple cardiac genes were up-regulated in GMTMM-HCFs after 1 wk of transduction (P1 HCFs, 2-y-old patient; $n = 3$). Representative data are shown in each panel. All data are presented as mean $\pm$ SD. $*P < 0.05$; $**P < 0.01$ vs. relevant control. (Scale bars: 100 μm.)

qRT-PCR after 1 wk of transduction. Of these 11 factors, only Myocd strongly induced Tnnt2 expression (Fig. 1F). Myocd also induced Nppa, but did not induce Ryr2 (ryanodine receptor 2). In contrast, Mesp1, Nkx2.5, and Pitx2c strongly induced Ryr2 expression (Fig. 1 G and H).

Consistent with our qRT-PCR results, FACS analysis and immunocytochemistry demonstrated that the addition of Myocd to GMT increased the expression of sarcomere proteins α-actinin and cTnT in HCFs compared with Mesp1. In contrast, threefold more cells exhibited spontaneous Ca^{2+} oscillations by transduction of GMTMesp1 compared with GMTMyocd after 4 wk of culture (Fig. S2 A–E and Movie S1).

We next investigated whether the addition of Mesp1, Nkx2.5, or Pitx2c to GMT and Myocd could induce multiple cardiac gene expression. We found that Nkx2.5 and Pitx2c inhibited Tnnt2 mRNA expression, but that addition of Mesp1 up-regulated all three cardiac genes (Fig. 1 I–K). Moreover, transduction of Gata4, Mef2c, Tbx5, Mesp1, and Myocd (GMTMM) up-regulated the expression of a panel of cardiac genes related to different functions, including sarcomere structure, ion channels, and transcription factors, compared with GMT or mock infection, suggesting a more comprehensive reprogramming by GMTMM than by GMT (Fig. 1L).
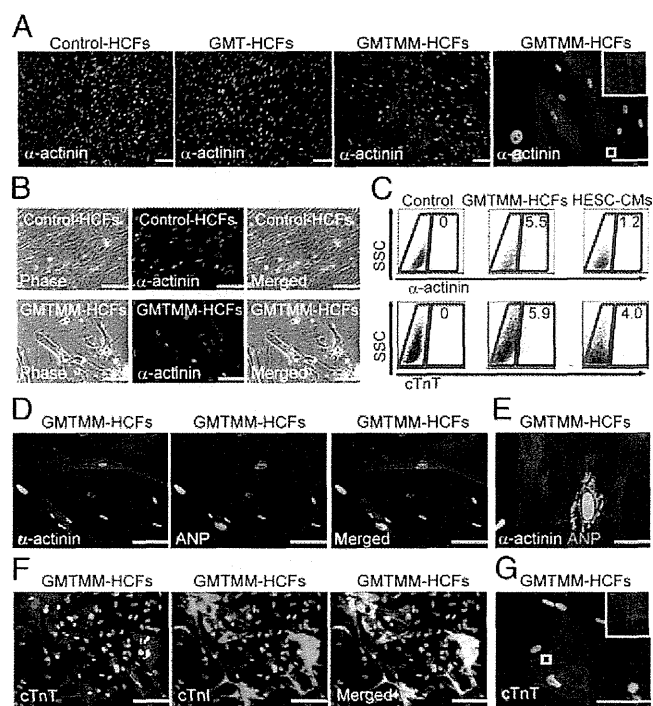

Fig. 2. Generation of cardiomyocyte-like cells from HCFs with GMTMM. (A) Immunostaining for α-actinin and DAPI in HCFs and GMT- or GMTMM-transduced HCFs at 4 wk after transduction (P1 HCFs, 3-y-old patient; $n = 4$). Note that GMTMM induced abundant and strong α-actinin expression. (Inset) High-magnification view of the area in the white box showing sarcomeric organization (see Fig. S1E for a positive control). (B) Morphology of mock- and GMTMM-infected HCFs by phase-contrast imaging and with α-actinin immunostaining (P1 HCFs, 57-y-old patient; $n = 3$). (C) Quantitative data of α-actinin$^+$ (P1 HCFs, 3-mo-old patient; $n = 3$) and cTnT$^+$ (P1 HCFs, 5-mo-old patient; $n = 3$) cells in GMTMM-HCFs and HESC-CMs ($n = 3$). (D and E) GMTMM-HCFs expressed both α-actinin and ANP at 4 wk after transduction (P1 HCFs, 5-y-old patient; $n = 2$). ANP was expressed at the perinuclear site. (F and G) Induced cardiomyocyte-like cells expressed cTnT and cTnI at 8 wk after GMTMM transduction (P1 HCFs, 5-y-old patient; $n = 2$). (Inset) High-magnification view representing the area in the white box. Representative data are shown in each panel. (Scale bars: 100 μm in A, B, D, F, and G; 50 μm in E.)

($>90\%$) using the pantropic retrovirus from PLAT-GP cells, and used this virus in subsequent experiments (Fig. 1 C–E).

We next transduced HCFs with a mixture of GMT retroviruses. The GMT overexpression induced very few α-actinin$^+$ cells, suggesting that this mixture is insufficient for human cardiac reprogramming (Fig. 2A). To identify reprogramming factors, we screened an additional 11 factors for use in combination with GMT and analyzed the induction of multiple cardiac genes by

Wada et al.

Gata4, Mef2c, Tbx5, Mesp1, and Myocd Induce Cardiac-Specific Proteins and Sarcomeric Structures in HCFs. We next used immunocyto-chemistry to examine whether cardiac proteins were expressed in HCFs by GMTMM. We found that more GMTMM-transduced HCFs (GMTMM-HCFs) expressed α-actinin with higher intensity compared with GMT, and that the α-actinin^{+} cells had sarcomere-like structures after 4 wk of culture (Fig. 2A). Morphologically, mock-infected HCFs were spindle-shaped, whereas GMTMM-HCFs appeared thicker and refractive on phase-contrast micros-copy, with a polygonal or rod-like shape (Fig. 2B). FACS analysis demonstrated that approximately 5% of the GMTMM-HCFs ex-pressed the endogenous cardiac proteins α-actinin and cTnT (Fig. 2C). In addition to α-actinin, the GMTMM-HCFs expressed several cardiomyocyte-specific proteins, including atrial natriuretic peptide (ANP), cTnT, cTnI, and connexin 43 (Cx43), at similar levels as those in the human ES cell-derived cardiomyocytes (HESC-CMs) (Fig. 2 D–G and Figs. S1E and S2F). Approximately 40% of α-actinin^{+} cells expressed ANP, and most cTnT^{+} cells expressed cTnI, another cardiomyocyte-specific sarcomere protein (Fig. 2 D–G). The addition of Nkx2.5 reduced cTnT expression, confirming the qRT-PCR results (Fig. 1I and Fig. S2G). These findings suggest that GMTMM induces multiple cardiac proteins and cardiomyocyte-like structures in HCFs.

GMTMM Up-Regulates a Broad Range of Cardiac Genes and Suppresses Fibroblast Gene Expression. Next, to decipher the global transcrip-tional changes induced by GMTMM transduction, we investigated the gene expression profiles of HCFs, GMTMM-HCFs, and hearts by microarray analyses. We analyzed the mRNA expression of GMTMM-HCFs after 1 wk of infection at the early reprog-ramming stage, because we were not able to isolate human iCM populations from GMTMM-HCFs, and the percentage of iCMs relative to the total number of GMTMM-HCFs decreased over time owing to their loss of proliferative capacity. Among the 24,462 genes analyzed, 1,432 genes were differentially expressed by more than twofold between HCFs and GMTMM-HCFs, with 1,018 genes up-regulated and 414 genes down-regulated in GMTMM-HCFs (Fig. 3A). The genes up-regulated in GMTMM-HCFs were significantly enriched in hearts compared with HCFs ($P = 1.6E\text{-}86$) and, conversely, the down-regulated genes were enriched in fibro-blasts ($P = 4.7E\text{-}67$) (Fig. 3B).

Gene Ontology (GO) analyses demonstrated that the genes up-regulated in GMTMM-HCFs were enriched related to car-diomyocyte functions, whereas the down-regulated genes were enriched for fibroblast functions, including cell division, mitotic cell cycle, cell proliferation, and cell adhesion (Fig. 3C). Heat-map and qRT-PCR analyses of a panel of cardiac and fibro-blast genes in HCFs, GMTMM-HCFs, and hearts revealed that GMTMM up-regulated cardiac genes and concomitantly sup-pressed fibroblast gene expression (Fig. 3 D and E).

GMTMM Directly Induces Cardiomyocyte-Like Cells from Fibroblasts. We next asked whether GMTMM also could induce smooth muscle cells or endothelial cells from fibroblasts. Microarray and qRT-PCR analyses revealed induction of smooth muscle genes, but not endothelial cell genes, in GMTMM-HCFs (Fig. 4 A and B). Consistent with this finding, immunostaining demonstrated that CD31 was not expressed in GMTMM-HCFs, whereas cal-ponin and smooth muscle myosin heavy chain (SMMHC), mark-ers for smooth muscle cells, and α-smooth muscle actin (α-SMA), a marker of smooth muscles and embryonic cardiomyocytes (19), were induced by GMTMM transduction (Fig. 4 C and D and Fig. S3A). Coimmunostaining revealed that α-actinin^{+} cells expressed α-SMA but not SMMHC, suggesting that the iCMs were relatively immature cardiomyocytes without a mixed phenotype between cardiomyocytes and smooth muscle cells (Fig. 4 E–G).

We next examined the reprogramming kinetics by analyzing the cardiomyocyte and smooth muscle cell gene induction by
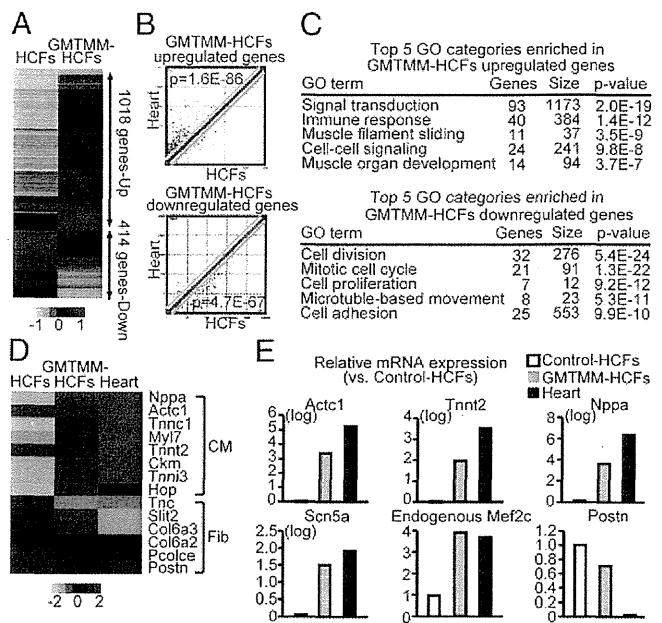

Fig. 3. GMTMM up-regulates cardiac genes and down-regulates fibroblast genes. (A) Heatmap image of microarray data, illustrating differentially expressed genes between control-HCFs and GMTMM-HCFs (P1 HCFs, 65-y-old patient; $n = 1$). The scale is –1 to +1 in log10. Red indicates increased ex-pression, and green indicates decreased expression. "Up" indicates the genes up-regulated in GMTMM-HCFs compared with HCFs, and "down" indicates the genes down-regulated by GMTMM transduction compared with HCFs. (B) Paired scatterplots of the up-regulated and down-regulated genes in the GMTMM-HCFs. The up-regulated genes were significantly enriched in heart, whereas the down-regulated genes were enriched in HCFs. (C) GO term analyses of the up-regulated and down-regulated genes in GMTMM-HCFs compared with HCFs. The top five GO categories are shown. (D) Heatmap image of gene expression of cardiomyocyte (CM)- and fibroblast (Fib)-enriched genes in HCFs, GMTMM-HCFs, and heart. The scale is –2 to +2 in log10. (E) mRNA expression in HCFs, GMTMM-HCFs, and heart were determined by qRT-PCR (P1 HCFs, 2-y-old patient; $n = 3$). Data were normalized against the control-HCF values. All data are presented as mean, and the scales are log10 in Actc1, Tnnt2, Nppa, and Scn5 mRNA expression (E).

qRT-PCR. The cardiomyocyte-specific genes *Actc1*, *Nppa*, *Ryr2*, and *Tnnt2* and smooth muscle-specific gene *Myh11* were up-regulated from 4 d and subsequently down-regulated at 28 d by GMTMM, because these reprogrammed myocytes were not pro-liferative (Fig. 4H). We then performed 5-ethynyl-2′-deoxyuridine (EdU) incorporation assays to determine whether the conversion of fibroblasts to cardiomyocyte-like and smooth muscle-like cells is mediated through a mitotic cell state. A 2-hr pulse labeling of EdU after 4 or 24 h of transduction demonstrated significantly reduced cell proliferation in the GMTMM-HCFs, consistent with the GO term analysis results (Fig. S3 B–D). Long-term pulse labeling of EdU throughout a 4-wk culture period dem-onstrated that a vast majority of α-actinin[+] and SMMHC^{+} cells did not express EdU. These results suggest that most induced cardiac and smooth muscle cells do not pass through a mitotic cell state and start to express cardiac or smooth muscle genes from the early stage of reprogramming (Fig. 4 I–K).

Induced Cardiomyocyte-Like Cells Exhibit Action Potentials and Contractile Ability in Coculture with Murine Cardiomyocytes. To determine whether the iCMs derived from HCFs have the func-tional properties of cardiomyocytes, we analyzed intracellular Ca^{2+} oscillations after 4 wk of culture. We did not observe Ca^{2+} oscillations in mock-infected HCFs. In contrast, approximately 1% of GMTMM-HCFs showed spontaneous Ca^{2+} oscillations, albeit
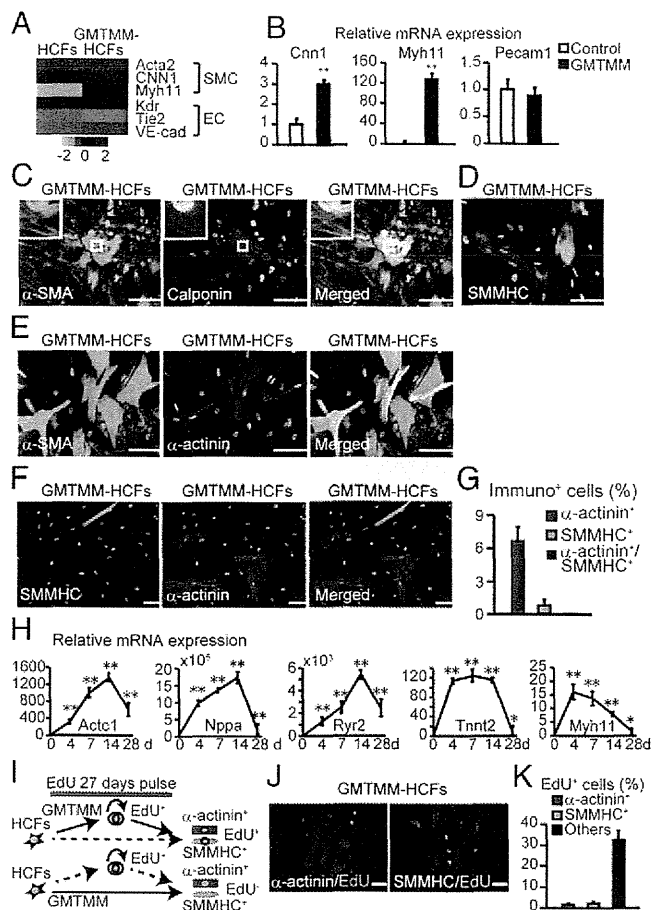
cells contracted synchronously with surrounding cardiomyocytes; however, conditioned media from rat cardiomyocytes did not induce spontaneous contraction in the GMTMM-transduced cells. The beating iCMs revealed periodic Ca oscillations and action potentials (APs) similar to those of HESC-CMs (Fig. 5 *F–J* and Movie S4) (20). Atrial-like APs were the most frequently recorded in the HCF-iCMs ($n = 27$; 0 nodal type, 19 atrial type, and 8 ventricular type) (Fig. 5*J*). Of note, we injected Alexa Fluor 568 dye into the patched cells and confirmed that the recorded electrical activities came from the GMTMM/GFP$^+$ iCMs (Fig. 5*H*).

Next, to investigate cell fusion events, we transduced GMTMM and DsRed retrovirus mixtures into the HCFs and cocultured with GFP-labeled cardiomyocytes. Cellular contraction was apparent in DsRed$^+$ cells but not in DsRed$^+$/GFP$^+$ cells, suggesting that cell

Fig. 4. Generation of induced cardiomyocyte-like cells is not mediated through mitotic cells. (*A*) Heatmap image of gene expression of smooth muscle cell (SMC)- and endothelial cell (EC)-enriched genes in HCFs and GMTMM-HCFs (P1 HCFs, 65-y-old patient; $n = 1$). The scale is −2 to +2 in log10. (*B*) mRNA expression in control-HCFs and GMTMM-HCFs as determined by qRT-PCR (P1 HCFs, 2-y-old patient; $n = 3$). (*C*) Coimmunostaining for α-SMA and calponin in the GMTMM-HCFs (P1 HCFs, 50-y-old patient, $n = 3$). (*D*) Immunostaining for SMMHC in the GMTMM-HCFs (P1 HCFs, 80-y-old patient; $n = 3$). See also Fig. S1*E*. (*E*) Coimmunostaining for α-SMA and α-actinin in the GMTMM-HCFs (P1 HCFs, 5-mo-old patient; $n = 3$). (*F* and *G*) Double immunostaining for SMMHC and α-actinin in the GMTMM-HCFs, along with quantitative data for α-actinin$^+$ cells, SMMHC$^+$ cells, and α-actinin$^+$/SMMHC$^+$ cells (P1 HCFs, 5-mo-old patient; $n = 3$). (*H*) Time course of mRNA expression in GMTMM-HCFs at day 0 and at 4, 7, 14, and 28 d after infection, determined by qRT-PCR (P2 HCFs, 6-y-old patient; $n = 3$). (*I*) Schematic representation of EdU treatment on HCFs during reprogramming. (*J* and *K*) Immunocytochemistry for α-actinin and SMMHC in GMTMM-HCFs at 28 d after infection, coupled with EdU incorporation. The majority of immunopositive cells were negative for EdU. Quantitative data are shown in *K* (P1 HCFs, 1-y-old patient; $n = 3$). All data are presented as mean ± SD. *$P < 0.05$; **$P < 0.01$ vs. relevant control. (Scale bars: 100 μm.)

at a lower frequency compared with HESC-CMs (Fig. 5 *A–D* and Movies S2 and S3). Despite longer periods of culture, the GMTMM-HCFs did not beat spontaneously. Consequently, we next tested whether coculture with murine cardiomyocytes could induce further cardiac maturation. We transduced HCFs with GMTMM and GFP by separate vectors or GFP alone to mark the transduced cells, and after 1 wk of transduction, replated the cells onto neonatal rat cardiomyocytes. We found expression of cardiac markers, such as α-actinin, cTnT, and Cx43, in the GMTMM/GFP-HCFs, but not in the GFP-HCFs (Fig. 5*E* and Fig. S4 *A–C*). After 7 d of cocultivation, 5% of the GMTMM/GFP$^+$
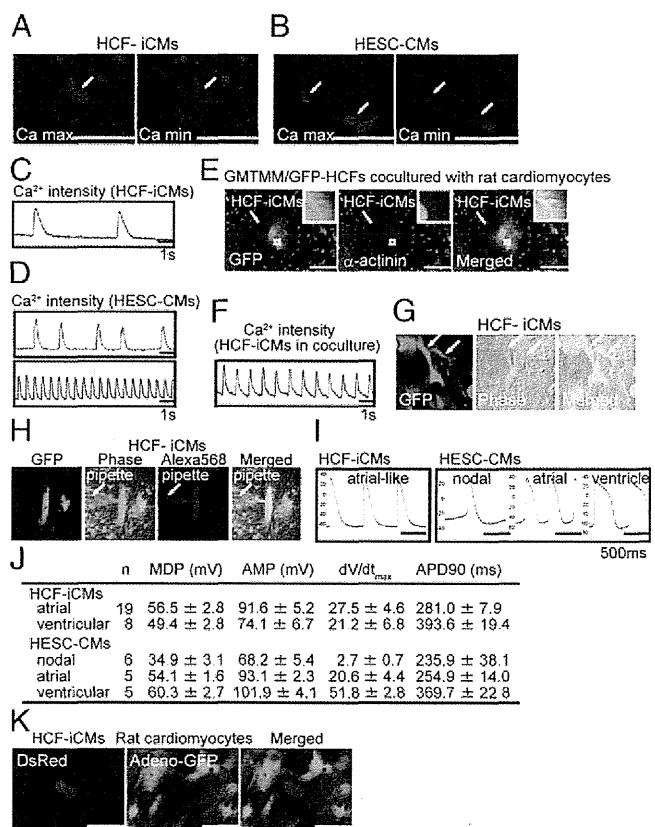

Fig. 5. Functional analyses of induced cardiomyocyte-like cells derived from HCFs. (*A* and *B*) Spontaneous Ca^{2+} oscillations were observed in HCF-iCMs (arrows in *A*) and HESC-CMs (arrows in *B*) (P1 HCFs, 5-mo-old patient; $n = 3$). Rhod-3 signals at maximum and minimum Ca^{2+} are shown. See also Movie S2. (*C* and *D*) HCF-iCMs showing spontaneous Ca^{2+} oscillation (*C*), similar to HESC-CMs (*D*; see also Movie S3). Rhod-3 intensity traces are shown. (*E*) Immunocytochemisty for α-actinin in the GMTMM/GFP-expressing HCF-iCMs (P2 HCFs, 57-y-old; $n = 2$) cocultured with rat cardiomyocytes. See also Fig. S4 *A–C*. (*F* and *G*) iCMs cocultured with rat neonatal cardiomyocytes showing Ca^{2+} oscillations (P1 HCFs, 77-y-old patient; $n = 2$). See also Movie S4. (*H*) APs recorded from iCMs (P1 HCFs, 57-y-old, 1-y-old, and 4-y-old patients; $n = 27$). The cells were injected with Alexa Fluor 568 to confirm that APs were obtained from the GFP$^+$ iCMs. (*I*) APs from HCF-iCMs and HESC-CMs. HESC-CMs revealed variable APs. (*J*) Summary of the measured AP parameters. MDP, maximum diastolic potential; AMP, amplitude; dV/dt, maximum rate of rise of AP; APD90, AP duration at 90% of repolarization. P1 HCFs from 57-y-old, 1-y-old, and 4-y-old patients were used for the experiments in the HCF-iCMs ($n = 27$). (*K*) HCF-iCMs (DsRed) cocultured with rat cardiomyocytes (GFP) (P1 HCFs, 17-y-old patient; $n = 4$). The DsRed$^+$ cell is beating without cell fusion. See also Fig. S4*D* and Movies S5 and S6. All data are presented as mean ± SEM. Representative data are shown in each panel. (Scale bars: 100 μm in *A*, *B*, *E*, and *K*.)

−133−

fusion was unlikely for cardiac differentiation in the coculture (Fig. 5K, Fig. S4D, and Movies S5 and S6).

Induction of Human Cardiomyocyte-Like Cells from Dermal Fibroblasts.
To exclude the possibility of contamination with rare CPCs or cardiomyocytes in our initial fibroblast populations, we tested whether HDFs also could be converted into iCMs by GMTMM. Neonatal foreskin dermal fibroblasts transduced with GMTMM expressed α-actinin, cTnT, and ANP and showed sarcomeric structures (Fig. 6 A and B). FACS analysis revealed that most HDFs were Thy1⁺/CD31⁻ fibroblasts, which also expressed cardiac genes after GMTMM transduction (Fig. S5 A and B). GMTMM-HDFs expressed cardiac-specific genes at levels comparable to GMTMM-HCFs on qRT-PCR analysis (Fig. 6C). Microarray analyses of HDFs, GMTMM-HDFs, and hearts demonstrated that the up-regulated genes in the GMTMM-HDFs were cardiac-enriched genes ($P = 1.2E\text{-}21$) and the down-regulated genes were fibroblast-enriched genes ($P = 1.5E\text{-}74$) (Fig. 6D and Fig. S5C). The top five GO categories enriched in the up-regulated genes included muscle contraction and muscle filament sliding (Fig. S5D). A panel of cardiac-specific genes, including *Actc1*, *Tnnc1*, *Nppa*, *Nppb*, *Myl7*, *Pln* (phospholamban), and *Ckm*, were up-regulated, whereas fibroblast genes *Col3a1*, *Col6a3*, *Col16a1*, *Ecm2*, *Ptn*, and *Tnc* were down-regulated in GMTMM-HDFs (Fig. 6E). We also observed that some GMTMM-HDFs exhibited cellular contraction and APs in coculture with murine cardiomyocytes ($n = 6$, nodal/atrial/ventricular type $= 0/2/4$) (Fig. 6 F, G, and K; Fig. S5 E and F; and Movie S7). These results exclude the possibility that the iCMs arose from contaminating cardiomyocytes or CPCs in initial fibroblast populations.

We next used a doxycycline-inducible system to assess the requirement for exogenous reprogramming factors in maintaining a cardiac phenotype in iCMs. We found that transduction efficiency was ~70%, and that transgene expression was instantly diminished by withdrawal of doxycycline, with complete loss after 10 d (Fig. S5G). Expression of GMTMM for 5 wk induced α-actinin and cTnT expression in HCFs (Fig. 6H and Fig. S5H). We then withdrew doxycycline after 1 wk, 10 d, or 2 wk of induction, and cultured the cells for 3 wk without doxycycline. Doxycycline removal after 1 wk and 10 d did not induce cardiac reprogramming, whereas 2 wk of induction maintained endogenous α-actinin and cTnT expression in the iCMs, and the cells exhibited APs in coculture with murine cardiomyocytes ($n = 7$; 0 nodal type, 7 atrial type, 0 ventricular type) (Fig. 6 H–K and Fig. S5I). These results suggest that the fibroblasts were stably converted into cardiomyocyte-like cells after 2 wk of GMTMM transduction.

Discussion

Here we demonstrate that human fibroblasts can be directly converted to cardiomyocyte-like cells by overexpression of defined factors. We found that a pantropic retrovirus was more efficient for transduction into HCFs compared with amphotropic or lentivirus/ecotropic retrovirus systems. Given that high transduction efficiency is critical for reprogramming, the pantropic retrovirus might be widely useful for direct reprogramming from difficult-to-infect cells (11).

Compared with mouse counterparts, induction of human iCMs required two additional factors, Mesp1 and Myocd. Generation of human iPSCs and neuronal cells also required different culture conditions or other transcription factors in addition to the mouse reprogramming factors (21, 22). Mesp1 is expressed in CPCs and programs nascent mesoderm toward a cardiovascular cell fate, whereas Myocd regulates the development of cardiomyocytes and smooth muscle cells (23–25). Islas et al. (26) recently reported that overexpression of Ets2 and Mesp1 reprogrammed HDFs into CPCs, and that the induced CPCs differentiated into immature cardiomyocytes. Mesp1 overexpression activated some of the
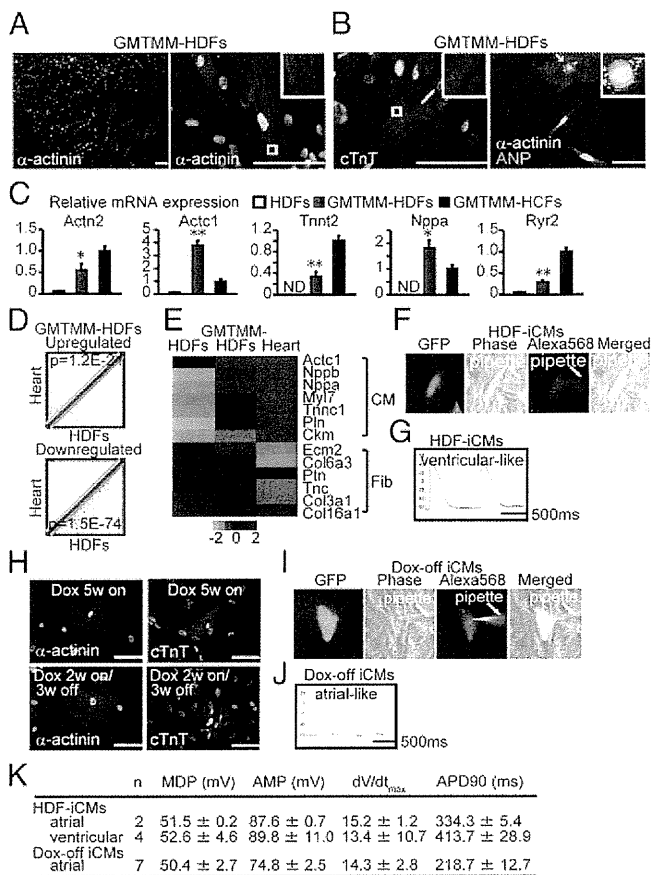

Fig. 6. GMTMM converts HDFs into cardiomyocyte-like cells. (A) Immunocytochemistry for α-actinin in GMTMM-HDFs at 4 wk after transduction (P3 HDFs; $n = 3$). (B) Immunocytochemistry revealing cTnT and ANP expression in GMTMM-HDFs (P3 HDFs; $n = 3$). (Insets) High-magnification views. (C) mRNA expression of cardiac genes in HDFs, GMTMM-HDFs (P3 HDFs), and GMTMM-HCFs as determined by qRT-PCR ($n = 3$). (D) Plots of gene expression up-regulated and down-regulated by more than twofold by GMTMM transduction in HDFs (P3 HDFs; $n = 1$). See also Fig. S5 C and D, heatmap image of microarray data and GO analyses. (E) Heatmap image of gene expression for cardiomyocyte (CM)- and fibroblast (Fib)-enriched genes in HDFs, GMTMM-HDFs, and heart. (F and G) APs recorded from GMTMM/GFP-expressing HDF-iCMs cocultured with rat cardiomyocytes (P3 HDFs; $n = 6$). The cells were injected with Alexa Fluor 568. Quantitative data are shown in K. See also Fig. S5 E and F and Movie S7. (H) (Upper) Immunostaining for α-actinin and cTnT in iCMs at 5 wk after Dox induction of the lentivirus. (Lower) Cells after 2 wk of Dox administration and 3 wk of Dox withdrawal (P1HCFs, 50-y-old patient; $n = 2$). See also Fig. S5 G–I. (I–K) APs recorded from iCMs at 2 wk after Dox withdrawal of the lentivirus (Dox-off iCMs) in coculture with cardiomyocytes (P1HCFs, 6-y-old patient; $n = 7$). Quantitative data are shown in K. Representative data are shown in each panel. Data are presented as mean ± SD in C and as mean ± SEM in K. *$P < 0.05$; **$P < 0.01$ vs. GMTMM-transduced HCFs. (Scale bars: 100 μm in A, B, and H.)

core cardiac transcription factors but failed to convert fibroblasts to CPCs. Given that their induced CPCs were highly replicative cells, the route of cardiac induction by Ets2/Mesp1 differed from that by GMTMM. More recently, Nam et al. (27) reported that overexpression of Gata4, Hand2, Tbx5, Myocd, miR-1, and miR-133 reprogrammed human fibroblasts into cardiac-like myocytes. Consistent with our results, they also found that neither of the mouse reprogramming factors GHMT or GMT was sufficient for cardiac reprogramming in human fibroblasts, and that the addition of Myocd significantly increased the expression of cardiac sarcomeric proteins. In addition, they reported that Hand2 was critical for inducing tropomyosin and cTnT in HDFs, and that

−134−

the addition of miR-1 and 133 further improved cardiac reprogramming and eliminated the requirement for Mef2c.

In their study, by transduction using the six factors, 13% of adult HCFs expressed cTnT and a small subset of the cells exhibited spontaneous contractions after 11 wk of culture, suggesting greater reprogramming efficiency than with GMTMM. However, the functional properties of the induced cardiac-like myocytes remain unclear, and further investigation may be needed to clarify this point. Myocd overexpression induces smooth muscle cells from fibroblasts by forming transcriptional complexes with Srf and promotes cardiomyocyte differentiation by interacting with Gata4 and Tbx5 (28–30). Stoichiometry of transcription factors might determine the cell fate of GMTMM-transduced cells to iCMs or smooth muscle-like cells in our study. As demonstrated by the fact that addition of Myocd up-regulated sarcomeric genes and Mesp1 induced intracellular Ca^{2+} oscillations, Myocd and Mesp1 differentially regulate cardiac gene expression in human cardiac reprogramming.

The human iCMs generated by GMTMM seem to be relatively immature cardiomyocytes, as indicated by their cell morphology, expression of embryonic cardiomyocyte marker α-SMA, and slow Ca^{2+} oscillations. Compared with mouse iCMs, human iCMs require coculture with murine cardiomyocytes to differentiate into beating cardiomyocytes. In this sense, the human iCMs may be similar to the early stage of embryonic cardiomyocytes before the start of contraction. Alternatively, the cells might be partially reprogrammed cardiomyocytes, much like the pre-iPSCs that can become fully pluripotent with additional stimuli.

Although the iCMs expressed a panel of cardiac-specific genes, their similarity of human iCMs to bona fide cardiomyocytes remained unclear. To address this question, we attempted to FACS-sort iCM populations using a fluorescent dye that labels mitochondria to selectively mark cardiomyocytes in ESC culture (31); however, we could not use this dye owing to the abundant labeling of mitochondria in the nonconverted HCF population. Further study is needed to thoroughly optimize conditions for human iCM generation and maturation and characterize the properties of iCMs.

It is possible that the immature iCM phenotypes could reflect the low percentage of iCMs and low cell–cell contact in the heterogeneous culture, and that enrichment of iCMs may enhance cardiac reprogramming. Given that secreted proteins, electrical and mechanical stimulation, and cell–cell contact might promote cardiac differentiation and reprogramming in the co-culture, the in vitro system might represent a valuable platform for screening such key factors. From a practical standpoint, GMTMM may be sufficient human cardiac reprogramming factors, considering that the in vivo environment might be more permissive than culture dishes for reprogramming (7, 13). Further in vitro and in vivo studies are needed to facilitate application of this technology in potential regenerative therapies.

Materials and Methods

Human atrial tissues were obtained from 36 patients undergoing cardiac surgery (age 1 mo to 80 y; average age, 35 y) with informed consent in conformation with the guidelines of the Keio University Ethics Committee. HCFs were obtained following the mouse protocol as detailed in *SI Materials and Methods*. Human neonatal foreskin dermal fibroblasts (DS Pharma Biomedical) were cultured in DMEM containing 10% FBS. All experiments were performed using fibroblasts of early passage number (P1–P3). The Keio Centre for Clinical Research approved all of the experiments in this study (20100131). Isolation of human fibroblasts, cell culture, retroviral and lentiviral infection, FACS analysis, immunocytochemistry, qRT-PCR, DNA microarray, calcium imaging, and patch clamp electrophysiology are described in *SI Materials and Methods*.

Note Added in Proof. Nam et al. (27) reported that overexpression of Gata4, Hand2, Tbx5, Myocd, miR-1, and miR-133 reprogrammed human fibroblasts into cardiac-like myocytes. We found that a different combination of cardiac reprogramming factors– Gata4, Mef2c, Tbx5, Mesp1, and Myocd–also reprogrammed human fibroblasts into cardiomyocyte-like cells. Our induced cardiomyocytes did not beat spontaneously, but matured to exhibit action potentials and contract synchronously in coculture with murine cardiomyocytes.

1. Zhou Q, Brown J, Kanarek A, Rajagopal J, Melton DA (2008) In vivo reprogramming of adult pancreatic exocrine cells to beta-cells. *Nature* 455(7213):627–632.
2. Vierbuchen T, et al. (2010) Direct conversion of fibroblasts to functional neurons by defined factors. *Nature* 463(7284):1035–1041.
3. Sekiya S, Suzuki A (2011) Direct conversion of mouse fibroblasts to hepatocyte-like cells by defined factors. *Nature* 475(7356):390–393.
4. Lujan E, Chanda S, Ahlenius H, Südhof TC, Wernig M (2012) Direct conversion of mouse fibroblasts to self-renewing, tripotent neural precursor cells. *Proc Natl Acad Sci USA* 109(7):2527–2532.
5. Szabo E, et al. (2010) Direct conversion of human fibroblasts to multilineage blood progenitors. *Nature* 468(7323):521–526.
6. Ieda M, et al. (2010) Direct reprogramming of fibroblasts into functional cardiomyocytes by defined factors. *Cell* 142(3):375–386.
7. Song K, et al. (2012) Heart repair by reprogramming non-myocytes with cardiac transcription factors. *Nature* 485(7400):599–604.
8. Jayawardena TM, et al. (2012) MicroRNA-mediated in vitro and in vivo direct reprogramming of cardiac fibroblasts to cardiomyocytes. *Circ Res* 110(11):1465–1473.
9. Protze S, et al. (2012) A new approach to transcription factor screening for reprogramming of fibroblasts to cardiomyocyte-like cells. *J Mol Cell Cardiol* 53(3):323–332.
10. Chen JX, et al. (2012) Inefficient reprogramming of fibroblasts into cardiomyocytes using Gata4, Mef2c, and Tbx5. *Circ Res* 111(1):50–55.
11. Srivastava D, Ieda M (2012) Critical factors for cardiac reprogramming. *Circ Res* 111(1):5–8.
12. Inagawa K, et al. (2012) Induction of cardiomyocyte-like cells in infarct hearts by gene transfer of Gata4, Mef2c, and Tbx5. *Circ Res* 111(9):1147–1156.
13. Qian L, et al. (2012) In vivo reprogramming of murine cardiac fibroblasts into induced cardiomyocytes. *Nature* 485(7400):593–598.
14. Hansson EM, Chien KR (2012) Reprogramming a broken heart. *Cell Stem Cell* 11(1):3–4.
15. Palpant NJ, Murry CE (2012) Regenerative medicine: Reprogramming the injured heart. *Nature* 485(7400):585–586.
16. Inagawa K, Ieda M (2013) Direct reprogramming of mouse fibroblasts into cardiac myocytes. *J Cardiovasc Transl Res* 6(1):37–45.
17. Takahashi K, et al. (2007) Induction of pluripotent stem cells from adult human fibroblasts by defined factors. *Cell* 131(5):861–872.
18. Kitamura T, et al. (2003) Retrovirus-mediated gene transfer and expression cloning: Powerful tools in functional genomics. *Exp Hematol* 31(11):1007–1014.
19. Kruithof BP, Van Den Hoff MJ, Tesink-Taekema S, Moorman AF (2003) Recruitment of intra- and extracardiac cells into the myocardial lineage during mouse development. *Anat Rec A Discov Mol Cell Evol Biol* 271(2):303–314.
20. He JQ, Ma Y, Lee Y, Thomson JA, Kamp TJ (2003) Human embryonic stem cells develop into multiple types of cardiac myocytes: Action potential characterization. *Circ Res* 93(1):32–39.
21. Pang ZP, et al. (2011) Induction of human neuronal cells by defined transcription factors. *Nature* 476(7359):220–223.
22. Yu J, et al. (2007) Induced pluripotent stem cell lines derived from human somatic cells. *Science* 318(5858):1917–1920.
23. Bondue A, et al. (2008) Mesp1 acts as a master regulator of multipotent cardiovascular progenitor specification. *Cell Stem Cell* 3(1):69–84.
24. Huang J, et al. (2012) Myocardin regulates BMP10 expression and is required for heart development. *J Clin Invest* 122(10):3678–3691.
25. Hoofnagle MH, et al. (2011) Myocardin is differentially required for the development of smooth muscle cells and cardiomyocytes. *Am J Physiol Heart Circ Physiol* 300(5):H1707–H1721.
26. Islas JF, et al. (2012) Transcription factors ETS2 and MESP1 transdifferentiate human dermal fibroblasts into cardiac progenitors. *Proc Natl Acad Sci USA* 109(32):13016–13021.
27. Nam YJ, et al. (2013) Reprogramming of human fibroblasts toward a cardiac fate. *Proc Natl Acad Sci USA* 110(14):5588–5593.
28. Oh J, et al. (2004) Target gene-specific modulation of myocardin activity by GATA transcription factors. *Mol Cell Biol* 24(19):8519–8528.
29. Wang C, Cao D, Wang Q, Wang DZ (2011) Synergistic activation of cardiac genes by myocardin and Tbx5. *PLoS ONE* 6(8):e24242.
30. Wang Z, Wang DZ, Pipes GC, Olson EN (2003) Myocardin is a master regulator of smooth muscle gene expression. *Proc Natl Acad Sci USA* 100(12):7129–7134.
31. Hattori F, et al. (2010) Nongenetic method for purifying stem cell-derived cardiomyocytes. *Nat Methods* 7(1):61–66.
32. Ieda M, et al. (2009) Cardiac fibroblasts regulate myocardial proliferation through beta1 integrin signaling. *Dev Cell* 16(2):233–244.

–135–